The Cochlear Labyrinth of Krapina Neandertals

By

Michaela Beals

Submitted to the graduate degree program in Anthropology and the Graduate Faculty of the University of Kansas in partial fulfillment of the requirements for the degree of Master of Arts.

Chairperson, Dr. David Frayer

Committee member, Dr. Cheryl Hill

Committee member, Dr. Alan Redd

Committee member, Dr. John Ferraro

Date Defended: April 6, 2012

The Thesis Committee for Michaela Beals

certifies that this is the approved version of the following thesis:

The Cochlear Labyrinth of Krapina Neandertals

Chairperson, Dr. David Frayer

Date approved: April 6, 2012

Abstract

This study presents measurements of the cochlear labyrinth of Krapina Neandertals based on ultra high-resolution computed tomography. The cochlea, a membranous, fluid-filled structure, houses the sensory end organ of the auditory system. Located within the inner ear, the cochlea occupies a spiral shaped cavity within the bony labyrinth of the petrous bone. The close anatomical relationship between the membranous cochlea and the bony cochlear labyrinth allows for the determination of cochlear size from fossil specimens. Recent studies with extant primate taxa suggest that cochlear labyrinth volume is functionally related to the range of audible frequencies. Specifically, cochlear volume is negatively correlated with both the high and low frequency limits of hearing so that the smaller the cochlea, the higher the range of audible frequencies. This study shows that the Krapina Neandertals' cochlear volumes are similar to modern *Homo sapiens* and larger than chimpanzee and gorilla cochlear volumes. Although the nature of the relationship between cochlear volume and hearing abilities remains speculative, the measured cochlear volume in Krapina Neandertals suggests they had a range of audible frequencies that is similar to the modern human range.

Acknowledgements

I would like to express my gratitude to my advisor, David Frayer, for his support and guidance throughout this project. I would also like to thank my other committee members, Cheryl Hill, Alan Redd, and John Ferraro, whose helpful suggestions greatly improved this thesis. In particular, thank you to Cheryl Hill for access to the comparative sample scans, for technical training, and for excellent advice regarding this thesis.

I also thank Jakov Radovčić of the Croatian Natural History Museum for access to the Krapina fossil specimens, and Gerhard Weber and the technicians at the microCT lab at the University of Vienna for creating the beautiful Neandertal scans.

My sincere thanks go my family and friends for their unconditional support. Finally, thank you to my husband, Dave, for listening to me, encouraging me, and marrying me.

Table of Contents

Abstract……………………………………………………………………………...…iii

Acknowledgements……………………………………………………………………iv

Chapter I: Overview of Anatomy and Physiology of the Ear……………………………………1

- The external ear…………………………………………………………………………1
- The middle ear…………………………………………………………………...…..2
- The inner ear…………………………………………………………………………....3
  - The vestibular system ………………………………………………………….4
  - The cochlea…………………………………………………………………………..4
- Cochlear mechanics and physiology of sound transmission……………………………...6

Chapter II: Comparative Hearing among Mammals……………………………………………9

- Basic measures ……………………..…………………………………………….....9
- Mammalian hearing sensitivity and frequency processing …………….………………..11
- Hearing sensitivity in primates……………………………………………………..11
- Generalized vs. specialized cochleae……………………………………………..…..12
- Predictions from gross cochlear morphology…………………………………………14

Chapter III: Evolution of Hearing…………………………..……………………………..17

- Fossil evidence: primates…………………………………….………………….….17
- Fossil evidence: hominids…………………………………………………………..18
- Auditory structures in Neandertals…………………………………………………20

Chapter IV: The Krapina Site…………………………………..……………...……….23

- Discovery and excavation of Krapina……………………………………………...23
- Stratigraphy and chronology……………………………………………………….25

Chapter V: The Current Study……………………………………………………………….28

Materials and methods…………………………………………………………..…29

Specimens and CT scanning……………………………………..……………29

Delimitation of the cochlea…………………………………………………....32

Segmentation, thresholding, and 3D reconstruction……………………………..34

Error and validation……………………………………………………………...37

Statistical analyses……………………………………………………….…37

Chapter VI: Results………………………………………………..……………..…….40

Qualitative analysis…………………………………………………………..……..40

Quantitative Analysis……………………………………………………………….42

Descriptive statistics…………………………………………….……………42

Nonparametric analyses….………………………………………………..…..43

Absolute cochlear volume……………………………………………..43

Scaled cochlear volume……………………………………………….....44

Linear regression………………………………………………………………46

Chapter VII: Discussion…………………………………………………………..……...48

Potential mechanisms for the relationship

between cochlear volume and hearing ability……………………………..49

Implications for ecology and communication of Neandertals…………………………..50

Future directions for the Krapina scans ………………………………………….......52

Summary………………………………………………………………………………...53

Bibliography……………………………………………………………………………….54

Appendices……………………………………………………………………………….59

List of Figures and Tables

Figure 1. The divisions of the ear……………………………………………………………1
Figure 2. The bony and membranous labyrinth……………………………………………..3
Figure 3. Cross section of a cochlear turn ………………………………………………..5
Figure 4. Travelling wave on an "unrolled" cochlea…………….………………………..7
Figure 5. Sound wave illustration……………………………………………………...…9
Figure 6. Primate audiograms………………………………………………………..…...12
Figure 7. Average audiogram for *Pan troglodyte* and *Homo sapiens* ………………………..19
Figure 8. Dr. Dragutin Gorjanović-Kramberger ..………………………………………....23
Figure 9. Successive slices from a chimpanzee petrosal…………………………….…..32
Figure 10. Successive slices through the petrosal of a Neandertal………………....……….33
Figure 11. Schematic representation of segmenting and 3D cochlear
reconstruction…………………………………………………………………….…36
Figure 12. Inner ear structures of Krapina 39.13…………………………………………...40
Figure 13. 3D reconstruction of gorilla, chimpanzee,
Neandertal, and modern human cochlear labyrinths……………..…………………….…..41
Figure 14. Neandertal cochlear labyrinth reconstructions………………………………...….43
Figure 15. Bivariate plot of log10 cochlear volume (mm^3) by log10 body mass (kg)………..…46

Table 1. Krapina Neandertal sample with inner ear preserved………………………….……30
Table 2. Comparative sample composition……………………………………………..……..31
Table 3. Number of cochlear turns………………………………………………………..… 42
Table 4. Absolute cochlear labyrinth volume……………………………………..………..42
Table 5. p-values for Mann-Whitney U-tests…………………………………………..….45
Table 6. Values of mean cochlear volume (mm^3) predicted by body mass (kg)………..…….47

Chapter I

Overview of Anatomy and Physiology of the Ear

The focus of this study, the cochlea, houses the sensory end organ of the auditory system. Although the cochlea is arguably the most important anatomical structure related to hearing within the temporal bone, an understanding of the various divisions of the entire ear is necessary in order to comprehend the relevant literature and to make well-informed inferences about the hearing abilities of fossil specimens. This section presents an overview of the gross anatomy and basic physiology of the three divisions of the ear.

The external ear

The external (or outer) ear, which consists of the pinna and external auditory canal (see Figure 1), gathers acoustic energy from the environment and directs it to the eardrum, or tympanic membrane. The shape of the external ear modifies the acoustic energy such that certain frequencies are selectively boosted. In humans, for

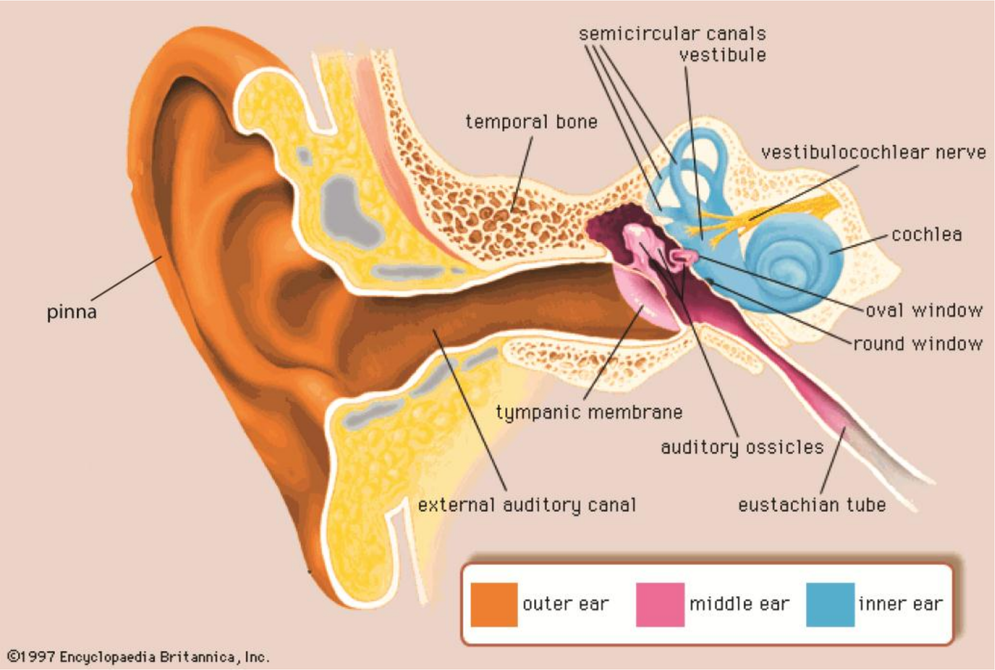

Fig. 1. The divisions of the ear. From www.brittanica.com

example, the external ear amplifies the sound pressure level 30- to 100- fold for frequencies between 2000 and 5000 Hertz Purves et al., 1997). Additionally, the frequency filtering properties of the pinna and concha provide cues for sound localization regarding the vertical elevation of a sound source (Purves et al., 1997).

The middle ear

Within the temporal bone, the middle ear comprises the tympanic membrane, the three tiny bones that make up the ossicular chain (malleus, incus, and stapes), the air-filled middle ear (or tympanic) cavity, a portion of the Eustachian (or pharyngotympanic) tube, and the two middle ear muscles (tensor tympani, and stapedius) (Rosowski, 1994). The tympanic membrane is the lateral boundary of the middle ear and articulates with the ossicular chain, specifically the manubrium of the malleus. Medially, the malleus articulates with the incus, the middle bone of the ossicular chain. The most medial ossicle, the stapes, attaches to the oval window of the inner ear via the annular ligament of the stapedial footplate. See Figure 1 for a depiction of the anatomy of the middle ear.

When acoustic energy collected by the external ear vibrates the tympanic membrane, the ossicular chain is also set into motion and transmits mechanical energy to the inner ear. The major function of the middle ear is to minimize the energy loss that would occur if sound energy in the air were to impinge directly on the inner ear fluids. Typically, when a sound travels from a low impedance medium, like air, to a much higher impedance medium, like water, only a small percentage (less than .01%) of the acoustic energy is transmitted across the boundary (Purves et al., 1997). In humans, the middle ear compensates for this loss by amplifying the sound pressure almost 200-fold by the time it arrives at the inner ear (Purves et al., 1997). For this reason, the middle ear is said to function as an impedance matching transformer, overcoming the impedance mismatch between air and fluid. This amplification is achieved by two mechanical processes: the lever action of the malleus and incus, and the focusing of force from the large area of the tympanic membrane onto the smaller area of the oval window (Purves et al., 1997).

The inner ear

The inner ear is a complex system of spaces and structures within the petrous portion of the temporal bone. It houses the sensory end organs of hearing (cochlea) and of balance (the semicircular canals, utricle, and saccule). The term bony labyrinth is used to describe the connected series of bony canals and cavities that contain both the auditory and vestibular systems. The bony labyrinth consists of a central cavity called the vestibule, a spiral tube called the cochlea, and three nearly circular channels called semicircular canals (see Figure 2). The footplate of the stapes articulates with the oval window, which is located in the bony wall of the vestibule. Slightly inferior to the oval window lies the round window. The spiral-shaped cochlea is located antero-inferiorly to the vestibule, and the three semicircular canals (superior, posterior, and lateral) are posterior to the vestibule.

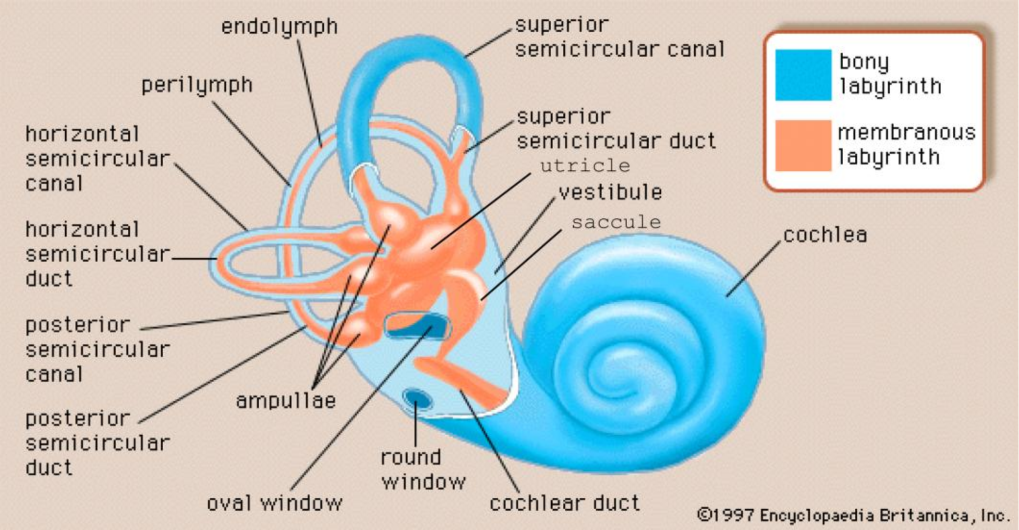

Fig. 2. The bony and membranous labyrinths.
From www.brittanica.com

The contours of the bony labyrinth are followed by the enclosed membranous labyrinth, which houses the sensory end organs of hearing and balance (see Figure 2). The membranous labyrinth contains two pouches, the utricle and saccule, located in the vestibule; three canals, one in each of the anterior, posterior, and lateral semicircular canals; and the cochlear duct of the cochlea. The entire membranous labyrinth is filled with a fluid called endolymph (intracellular fluid in composition), and is surrounded by the fluid of the bony labyrinth, which is called perilymph (extracellular fluid in composition) (Gelfand, 2004).

The vestibular system

The vestibular system is involved with balance or equilibrium. The membranous portion of the vestibular system in each ear contains five sensory receptors: one in each semicircular canal, one in the utricle, and one in the saccule. The receptors, or maculae, in the utricle and saccule are gravity sensitive and respond to linear acceleration (Gelfand, 2004). In other words, these receptors send nerve impulses to the brain via cranial nerve VIII when the head is moving in a straight line either horizontally or vertically, or stopping from a sustained linear motion. The ampullae are the sensory receptors of the semicircular canals and respond to angular or rotational acceleration. These sensory organs send nerve impulses to the brain when the head is turned from side to side or tilted up and down.

The cochlea

The snail-shaped cochlea houses the sensory end organ of the auditory system. Although the cochlea is often described as a free-standing structure, it is actually a spiral canal within the petrous portion of the temporal bone. The human cochlea is approximately 35 mm long from base to apex, and forms a somewhat cone-shaped spiral around its axis of rotation (Gelfand, 2004). It is widest at the base, where the diameter is about 9 mm, and narrows as it spirals toward the apex (Gelfand, 2004). The human cochlea makes approximately 2 and ¾ turns around its core, the modiolus (Gelfand, 2004).

The bony cochlea is divided into three chambers (scala media, scala vestibuli, and scala tympani) by the cochlear duct, a membranous tube. The cochlear duct originates within the vestibule between the oval and round windows and winds the length of the cochlea around the modiolus. It is attached medially to the osseous spiral lamina, a bony ramp-like shelf along the modiolus, and laterally by the spiral ligament. When viewed in cross-section, the cochlear duct is roughly triangular in shape and forms the central chamber, or scala media, within the bony canal (see Figure 3). The upper chamber, the scala vestibuli, is in contact with the footplate of the stapes at the oval window while the lower chamber, the scala tympani, terminates at the round window. The scalae vestibuli and tympani are joined together at the apex of the bony cochlea by the helicotrema. The scala media is bounded by membranes and contains endolymph like the rest of the membranous labyrinth. The other two scalae, however, are osseous cavities of the bony labyrinth that contain perilymph.

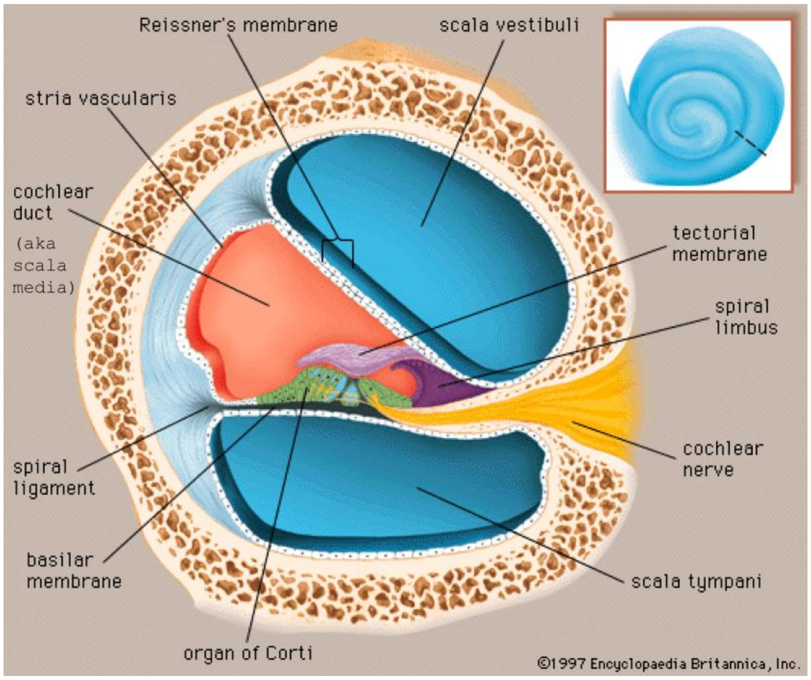

Fig. 3. Cross-section of a cochlear turn.
From www.britannica.com

Three structures, Riessner's membrane, the basilar membrane, and the stria vascularis, comprise the walls of the cochlear duct. Riessner's membrane forms the roof of the cochlear duct and is made up of connective tissue and epithelial cells. The lateral wall of the duct is formed by the stria vasularis, a capillary network that actively maintains the ionic composition of the endolymph and provides the blood supply to the sensory end organ of hearing (Echteler et al., 1994). The inferior border of the cochlear duct is the basilar membrane, a crucial structure for hearing.

The basilar membrane extends horizontally across the cochlear canal from the inferior border of the osseous spiral lamina to the spiral ligament, a thickening of the periosteum that lines the bony cochlea. The total width of the basilar membrane increases from base to apex in all species examined thus far (Echteler et al., 1994). In humans, the basilar membrane is approximately 32 mm long and becomes progressively wider from base (~.1 mm) to apex (~.5 mm) (Gelfand, 2004). The organ of Corti, the sensory end organ of hearing, is located superior to the basilar membrane.

Cochlear mechanics and physiology of sound transmission

The primary function of the cochlea is to act as frequency analyzer. Sound waves are collected from the external environment by the pinnae and propagated through the external auditory canal to the tympanic membrane. The vibrations of the tympanic membrane set the ossicular chain into motion, which causes the footplate of the stapes to move in a piston-like fashion against the oval window. The mechanical movements of the oval window produce hydraulic pressure fluctuations within the adjacent fluid-filled scala vestibuli. If the movements of the oval window are extremely slow, such as those at very low frequencies, displaced perilymph flows along the length of the scala vestibuli to the helicotrema where it is freely transmitted to the scala tympani. The perilymph then flows the length of the scala tympani to the round window and dissipates. In these instances, the helicotrema acts as an acoustic shunt to reduce the pressure difference across the cochlear duct. At higher acoustic frequencies, however, the pressure wave originating at the oval window develops too quickly to be dissipated by the flow of perilymph through the helicotrema. Thus, at these frequencies, the pressure difference between the scalae vestibuli and tympani causes displacement of the cochlear duct. The pattern of displacement of the mammalian cochlear duct is that of a travelling wave with several unique characteristics (Békésy, 1960). The wave always originates at the base of the cochlea and moves unidirectionally toward the apex. Moreover, the travelling wave exhibits a crest, or peak of maximum displacement, at a specific location along the cochlear duct and then quickly subsides. See Figure 4 for a depiction of a travelling wave along the basilar membrane. The location of the peak of the wave is determined by the frequency of the acoustic stimulus: high frequency stimulation causes maximum displacement closer to the base of the cochlear duct, and low

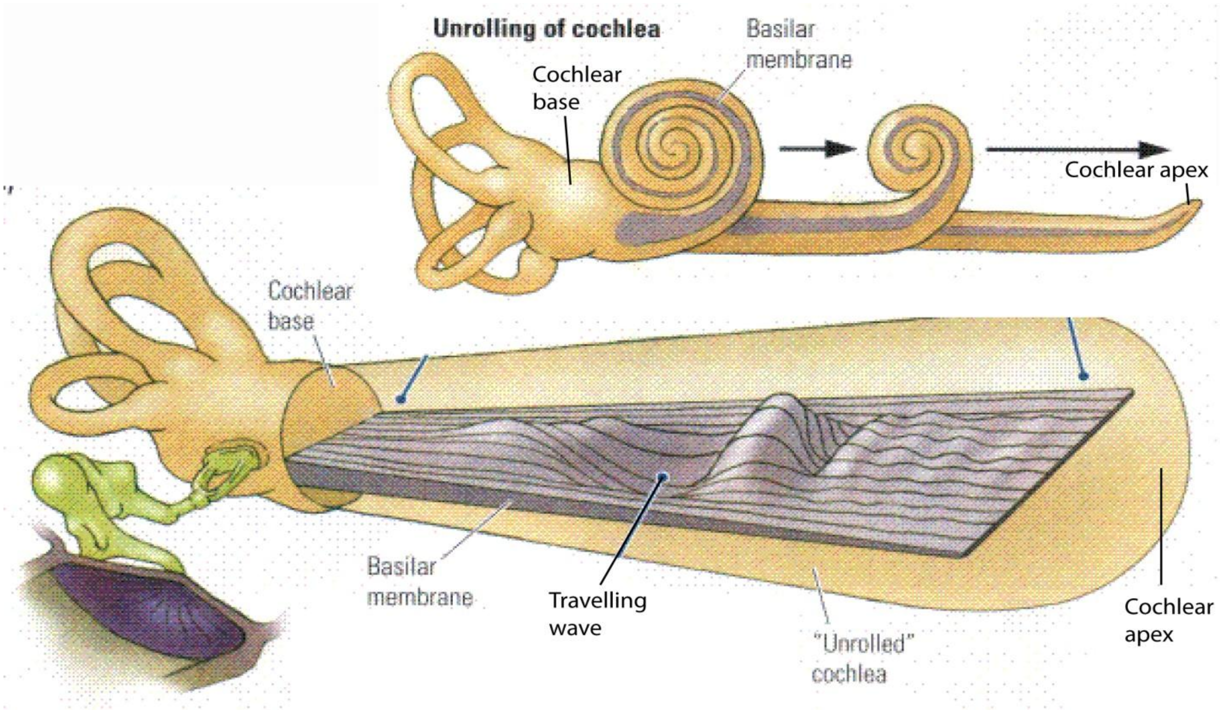

Fig. 4. Travelling wave on an "unrolled" cochlea.
Modified from http://www.cs.indiana.edu/~port/teach/641/audition.for.linguists.Sept1.html

frequency stimulation causes maximum displacement closer to the apex.

The differential displacement of the cochlear duct is caused by mass and stiffness gradients in the basilar membrane, as well as the force of the fluids that surround it (Békésy, 1960). The basilar membrane increases in width from base to apex, and this increase in width is accompanied by an increase in mass (Gelfand, 2004). Furthermore, the basilar membrane exhibits a stiffness gradient in the opposite direction from the mass gradient. Indeed, the basilar membrane is about 100 times stiffer at its base than at its apex (Gelfand, 2004). Thus, a certain degree of tuning is provided in the structure of the cochlear duct. With greater stiffness and less mass, the basal end of the cochlear duct is more attuned to higher frequencies, while decreased stiffness and increased mass render the apical end more responsive to lower frequencies.

Detailed physiology of the organ of Corti is beyond the scope of this study, but whenever the basilar membrane vibrates, small sensory hair cells inside the organ of Corti are bent by a shearing motion between the basilar membrane and the overlying tectorial membrane. This shearing bends the tiny processes, or stereocilia, that extend from the tip of the hair cells. When the stereocilia are bent in a particular direction, ion channels open and lead to voltage changes across the hair cell membrane. This electrical signal is sent via the cochlear branch of the vestibulocochlear nerve (cranial nerve VIII) to the brain, where it is interpreted as sound. The region of the basilar membrane that vibrates most vigorously stimulates the greatest number of hair cells in that area of the organ of Corti. These hair cells send nerve impulses to the brain, which recognizes the place on the basilar membrane (and thus the pitch of the tone) by the particular group of nerve fibers activated. The basilar membrane is therefore said to be tonotopically organized with different anatomical locations encoding sounds of differing frequency.

Chapter II

Comparative Hearing among Mammals

Since the gross dimensions of the cochlea are correlated with the range of audible frequencies for a given species, the cochlea can be used to make inferences about hearing capabilities (e.g. West, 1985, Echteler, 1994). This section presents a comparative review of mammalian hearing in order to better understand the form-function relationships between the morphology of the ear and hearing abilities.

Basic measures

The ear can distinguish different subjective aspects of a sound by detecting and analyzing different physical characteristics of the sound wave. Pitch and loudness are two commonly studied perceptual correlates of physical waveform properties. “Sound” actually refers to spherical shells of pressure waves generated by vibrating air molecules. The air molecules in the pressure waves are alternately dense (condensed) and sparse (rarefied) (see Figure 5).

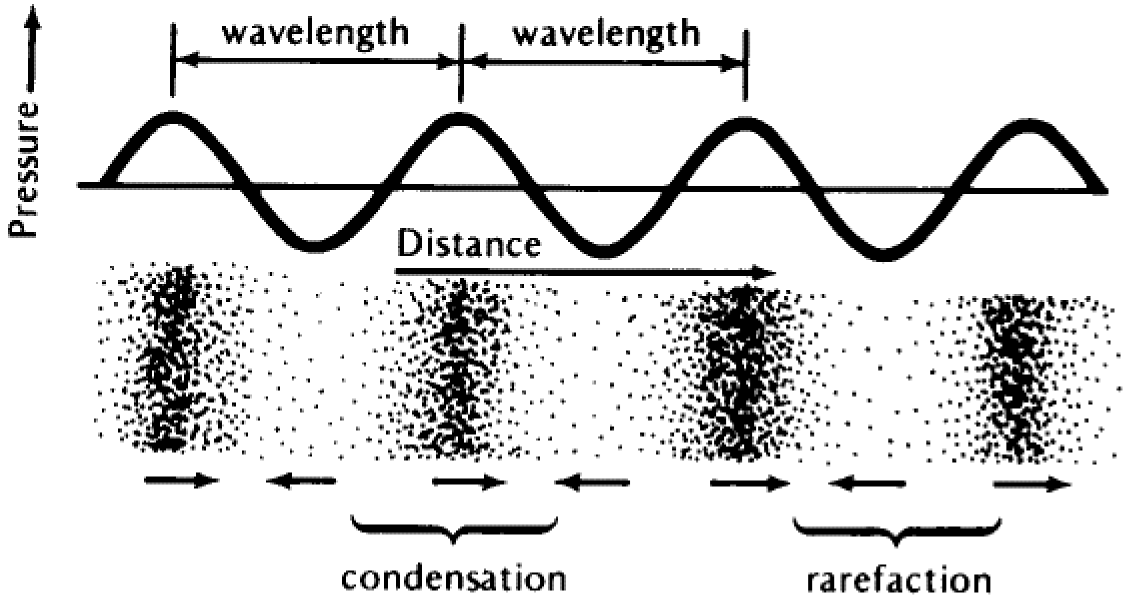

Fig. 5. Sound wave illustration. From http://www.economplex.org/complexity-science/complexity-emerges-from-simple-rules-demonstration-by-cymatics/

Frequency, measured in Hertz (Hz), is the number of these air rarefaction and compression cycles completed in one second (Purves et al., 1997). Pitch is the perceptual correlate of the frequency of sound waves. Loudness, on the other hand, is the perception of the intensity of sound. The intensity is the amount of pressure exerted by the sound wave on the tympanic membrane. Larger amplitude waves correspond to greater pressure on the tympanic membrane and greater perceived loudness of the sound (Purves et al., 1997). The intensity/pressure of sound is measured and reported in decibels (dB), a unit that expresses the relative magnitude of a sound on a logarithmic scale. Most acoustic measurements involved in hearing are made in terms of sound pressure level (rather than intensity level) and are reported in dB SPL (sound pressure level) (Gelfand, 2004). Frequency and intensity are important because they are the two main components of the audiogram, the standard graphical representation of humans' and other mammals' hearing capabilities. With frequency represented along the x-axis, and intensity represented along the y-axis, the audiogram plots the lowest sound level audible to the subject 50% of the time at each pure tone frequency. The audiogram line thus represents a series of thresholds; frequencies and intensities above the line can be detected and those below the line cannot. This standardized graph of hearing thresholds at different frequencies is useful in interspecific comparisons of hearing ability. Researchers often compare species based on the lowest (low-frequency limit) and highest (high-frequency limit) frequencies species can detect at a level of 60 dB SPL. The difference in octaves between high-frequency and low-frequency limits defines the audible hearing range. Two further parameters that are used for comparing species are the frequency of best hearing and the best sensitivity. The frequency of best hearing refers to the frequency (in Hz) at which the species has the lowest hearing threshold, and the best sensitivity refers to the measure of that threshold in decibels.

Mammalian hearing sensitivity and frequency processing

Compared to non-mammalian species, mammals have a broader audible frequency range due to their sensitivity to high-frequency sounds (Echteler et al., 1994). Additionally, mammals exhibit considerably more variation in hearing parameters than other vertebrates (Echteler et al., 1994). Still, there are three important generalizations that can be made with respect to mammalian hearing. First, most mammals, including humans, have the lowest thresholds within 10 dB of 0 dB SPL (sound pressure level) (Fay, 1994). Second, the highest audible frequency for a species is negatively correlated with body, head, and ossicle size (Rosowski, 1994) as well as with the distance between the ears (e.g. Heffner, 2004). In other words, larger mammals tend to have reduced high frequency limits compared to smaller mammals. For example, the high frequency limit for elephants is 10.5 kHz and the high frequency limit for mice is 79 kHz (West, 1985). Third, the frequency range of hearing is the hearing parameter that shows the most variation among mammals. The lower frequency limits range from 20 Hz to 10 kHz, and the upper frequency limits range from 11 kHz to 150 kHz (Fay, 1994). In general, wide differences in frequency range are consistent with the diversity of external, middle, and inner ear dimensions. The frequency limits of hearing are due to structural adaptations of the ear. Sensitivity at high frequencies is associated with external and middle ear structures that are small and stiff, whereas sensitivity at low frequencies is associated with large tympanic membrane areas and large, flexible middle ear spaces (Rosowski, 1994). Additional components of variation in hearing ranges are associated with the structure of cochlea.

Hearing sensitivity in primates

Primates show variation in hearing ability that generally follows phylogenetic patterns. Specifically, monkeys and apes (anthropoids) have better low-frequency sensitivity than lemurs and lorises (strepsirrhines), and within anthropoids, catarrhines (Old World monkeys and apes) have better low-frequency sensitivity than platyrrhines (New World monkeys) (Coleman and Colbert, 2010; see Coleman 2009 for a meta-analysis of primate audiogram studies). Lorises and lemurs exhibit the best high-frequency hearing among tested primates, whereas apes show reduced high-frequency sensitivity compared to monkeys. The audiograms of primates are generally the same shape, but shift along the frequency axis to lower frequencies from strepsirrhines to New World monkeys to Old World monkeys to apes, and finally, to humans (Heffner, 2004) (see Fig. 6). Additionally, the audiograms of monkeys and apes (except humans) often show two peaks of maximum sensitivity, while lemurs and lorises typically only have one peak in sensitivity. Lastly, humans are unique in showing maximal sensitivity in the region of 2-4 KHz, where many primates exhibit a mid-range decrease in sensitivity (see Coleman, 2009).

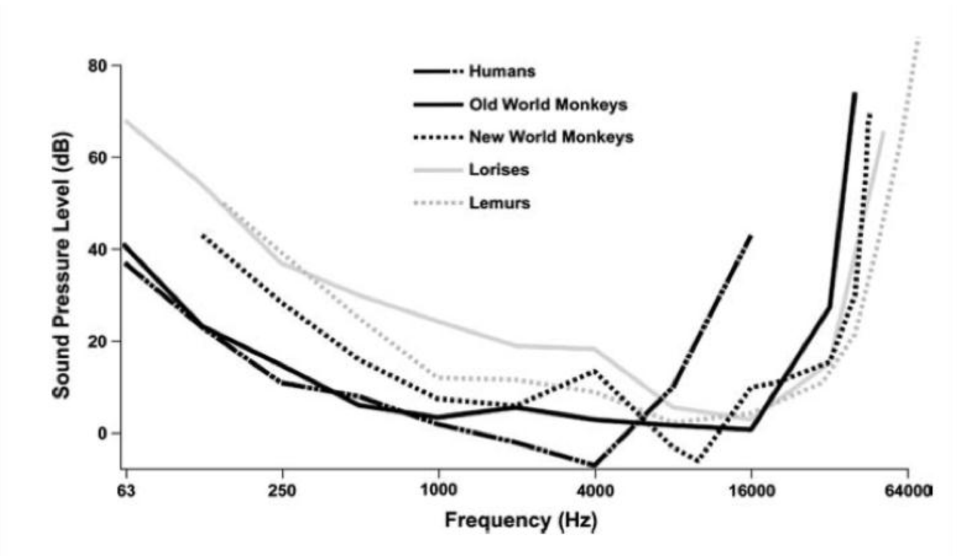

Fig. 6. Primate audiograms. Note that the shape is generally the same, but the audiograms shift along the frequency axis to lower frequencies from lemurs and lorises, to New World monkeys, to Old World monkeys, to humans.
From Coleman and Colbert, 2010 reproduced with permission from John Wiley & Sons

Generalized vs. specialized cochleae

Animals may be classified as having either generalized or specialized cochleae depending on the fits between predicted and actual frequency-place maps (Echteler et al., 1994). This distinction is important because it has implications for the applicability of predicting hearing abilities from morphology across species. Because the cochlear frequency-place map (i.e. the location of the peak of the travelling wave) is largely a result of the mass and stiffness of the basilar membrane, Békésy (1960) was able to determine frequency-place maps on dissected cochleae of several mammalian species. Greenwood (1990) later developed a function that models the predicted frequency-place maps based on basilar membrane parameters. Although later research has highlighted the importance of active physiological processes in frequency sensitivity, Békésy's and Greenwood's frequency-place maps remain generally valid (Fay, 1994). Research shows that mammals may be classified as having generalized or specialized cochleae depending on the fit between empirically determined frequency sensitivity and predicted cochlear frequency-place maps (Echteler et al., 1994). "Cochlear generalists" are those species for which the empirical data fit the predicted cochlear frequency-place map. "Cochlear specialists," on the other hand, are those species whose empirical frequency sensitivity is not well modeled by the predictive function (Echteler et al., 1994). The horseshoe bat (*Rhinolophus ferrumequinum*) and mole rat (*Spalax ehrenbergi*), for example, are termed "specialists" because their empirical place maps show abrupt slope transitions uncharacteristic of the usual frequency-place maps (Fay, 1992; Greenwood, 1961, 1990). These unique frequency-place maps reveal cochlear specializations that increase the acuity of frequency analysis in the high frequencies for the horseshoe bat and in the low frequencies for the mole rat (Echteler et al., 1994). These specializations are associated with unusual morphological features of the basilar membrane that are functional adaptations deviating from the general mammalian bauplan (Fay, 1994). Although cochlear map specializations enhance frequency resolution in specific frequency regions, not all species that hear particularly well in certain frequency ranges have specialized cochleae. Indeed, some species that hear particularly well at low (e.g. human), middle (e.g. cat), and high (e.g. rat and mouse) frequencies have generalized cochlear maps (Echteler et al., 1994). Still, the distinction between cochlear generalists and specialists is relevant because predictions regarding hearing capabilities from morphology typically do not hold for cochlear specialists.

Predictions from gross cochlear morphology

In general, accurate prediction of hearing capabilities from observable gross morphology of the cochlea is valuable to the comparative and evolutionary study of hearing. To date, the best understood relationship between ear structure and hearing ability is the correlation between basilar membrane length and frequency limits. West (1985) demonstrated that the length of the basilar membrane in terrestrial mammals is negatively correlated with both the high and low frequency limits of hearing. Specifically, shorter basilar membranes are associated with increases in high-frequency sensitivity and decreases in low-frequency sensitivity. As a result, terrestrial mammals with absolutely short basilar membrane lengths tend to have comparatively good high-frequency hearing, and mammals with absolutely long basilar membranes have comparatively good low-frequency hearing. Echteler et al. (1994) reported similar correlations between basilar membrane length and frequency limits for mammals with generalized cochleae. Mammals with specialized cochleae, like the horseshoe bat or mole rat, however, do not conform to the general mammalian trend (Echteler et al., 1994). Taken together, these data suggest that for most mammals, including primates, as basilar membrane length decreases, the range of hearing shifts to higher frequencies.

Kirk and Gosselin-Ildari (2009) propose that cochlear volume is functionally related to the range of audible frequencies in primates, either as a proxy for basilar membrane length or as an independent phenomenon. Specifically, cochlear volume is negatively correlated with both the high and low frequency limits of hearing. Thus, as cochlear volume increases, the range of audible frequencies shifts downward. Cochlear volume remains significantly correlated with the high-frequency limit of hearing even when body mass is held constant (Kirk and Gosselin-Ildari, 2009).

Recently, Coleman and Colbert (2010) investigated the functional morphology of the auditory system in a diverse sample of extant non-human primates. Measures of numerous structures from the external, middle, and inner ears indicate that low-frequency sensitivity is highly correlated with the size and shape of several auditory structures, including cochlear length, tympanic membrane area, stapedial footplate area, and the volume of the middle ear cavity. Cochlear length showed the strongest correlation with low-frequency sensitivity (Coleman and Colbert, 2010; Coleman, 2007). Although basilar membrane length is best estimated by measuring the length of the bony spiral lamina along the inner surface of the cochlear duct, the lamina is often incomplete in dried specimens and rarely present in fossils. Therefore, Coleman and Colbert (2010) measured the outer circumference of the cochlea from the round window to the helicotrema as a proxy for basilar membrane length.

Lastly, West (1985) concluded that there is a correlation between hearing range and the number of cochlear spirals. The number of cochlear turns in mammals ranges from 1.5 to 4.5 and does not seem to follow a phylogenetic pattern (see Ni et al., 2010). West (1985) noted a general trend among "cochlear generalists" that a greater number of turns is associated with a broader hearing range, independent of basilar membrane length. Manoussaki et al. (2008) however, suggest that the relevant characteristic regarding cochlear shape is not the number of cochlear turns but shape of the cochlear spiral. These researchers suggest that the cochlea's graded curvature from base to apex enhances low-frequency hearing by directing sound energy toward the apex of the cochlea, where low-frequency sounds are resolved. Manoussaki et al. (2008) demonstrated that the greater the curvature, or more specifically, the greater the ratio of the radii of curvature from the basal coil to the apical coil, the lower the low-frequency hearing limit for both terrestrial and aquatic mammals.

Chapter III

Evolution of Hearing

Studies examining the functional morphology of the cochlea not only increase our understanding of auditory patterns in extant taxa, but also lay the foundation for investigating the possible hearing capabilities of fossil specimens. This section discusses the small but growing body of evidence surrounding the evolution of hearing in extinct taxa. To date, the research is uneven with respect to taxa and auditory structures studied. This review discusses the relevant research pertaining to auditory function in Late Paleocene primates, Miocene primates, and hominids.

Fossil evidence: primates

Primates offer considerable fodder for studies of the evolution of hearing because of their relatively rich fossil record spanning the entire Cenozoic. Armstrong et al. (2011) examined the relationship between cochlear volume and body mass in extant non-primate euarchontoglirans (the supraordinal grouping to which all primates belong) and in two fossil specimens from the Late Paleocene (~60 mya). One of the fossils, *Labidolemur kayi*, is thought to be a non-primate euarchontogliran, while the other, *Carpolestes simpsoni*, is a stem primate. Armstrong et al. (2011) show that extant primates have significantly higher cochlear volumes relative to body mass than other euarchontoglirans. This suggests that an upward shift in relative cochlear volume has occurred over the course of primate evolution. Kirk and Gosselin-Ildari (2009) demonstrated in primates that increases in cochlear volume may be related to downward shifts in audible frequency range. Thus, it is possible that extant primates may have a lower range of hearing than closely related or ancestral non-primates.

In another recent study, Coleman et al. (2010) used high-resolution computed tomography to examine the auditory region of three fossil New World monkeys (*Homunculus, Dolicocebus, and Tremacebus*) from early Miocene deposits in Argentina dated to between 20 and 16.5 million years ago. Comparison with a diverse sample of extant taxa revealed that the extinct taxa share many characteristics with extant New World monkeys. Specifically, these similarities in morphology suggest that these fossil specimens likely had similar low-frequency sensitivity to extant South American monkeys (Coleman et al., 2010). This study suggests that good low-frequency sensitivity (when compared to other vertebrates) is a primitive platyrrhine trait that dates back to at least 20 million years ago.

Fossil evidence: hominids

Though cochlear volume data have not been examined in hominids, two ossicles from early hominids have been described – an incus from *Australopithecus robustus* (Rak and Clarke, 1979) and a stapes from *Australopithecus africanus* (Moggi-Cecchi and Collard, 2002). In their study, Moggi-Cecchi and Collard (2002) proposed a functional analysis of early hominid hearing from the preserved stapes found in association with a specimen (Stw 151) from Sterkfontein, South Africa. The researchers collected a number of measurements from the stapes and found that all values recorded for the Stw 151 stapes fall outside the range of variation in modern human samples. Specifically, the stapes has a small footplate area that falls within the great ape size range, but which is smaller than modern humans. Taxa with smaller stapedial footplate areas typically have enhanced high-frequency hearing, whereas taxa with large footplate areas are typically better at detecting low-frequency sounds (Rosowski, 1994). Thus, the small hominid stapes suggests that early hominids may have been more sensitive to high-frequency sounds than modern humans (Moggi-Cecchi and Collard, 2002).

Researchers have also investigated the ossicles of the middle ear of *Homo heidelbergensis*, the ancestor of both modern humans and Neandertals (Arsuaga et al., 1993). Martinez et al. (2004) used a comprehensive physical model to analyze the influence of skeletal structures on the acoustic filtering of the external and middle ear in five fossil humans from the Middle Pleistocene site of Sima de los Huesos (SH) in Atapuerca, Spain. Sound power transmission was also modeled for modern humans and chimpanzees to serve as comparisons for the fossil specimens.

The auditory capacities of modern humans and chimps exhibit clear differences. Chimpanzee audiograms show a W-shaped pattern characterized by two areas of high sensitivity at ~1 kHz and at 8 kHz, and an area of relatively low sensitivity from 2-4 kHz. Modern humans, on the other hand, show a U-shaped audiogram with the highest sensitivity from 2-4 kHz (see Figure 7). The results of the physical model show that the skeletal anatomy of the external and middle ear in the SH hominins is compatible with a human-like sound power transmission, clearly distinct from chimpanzees in the region around 4 kHz.

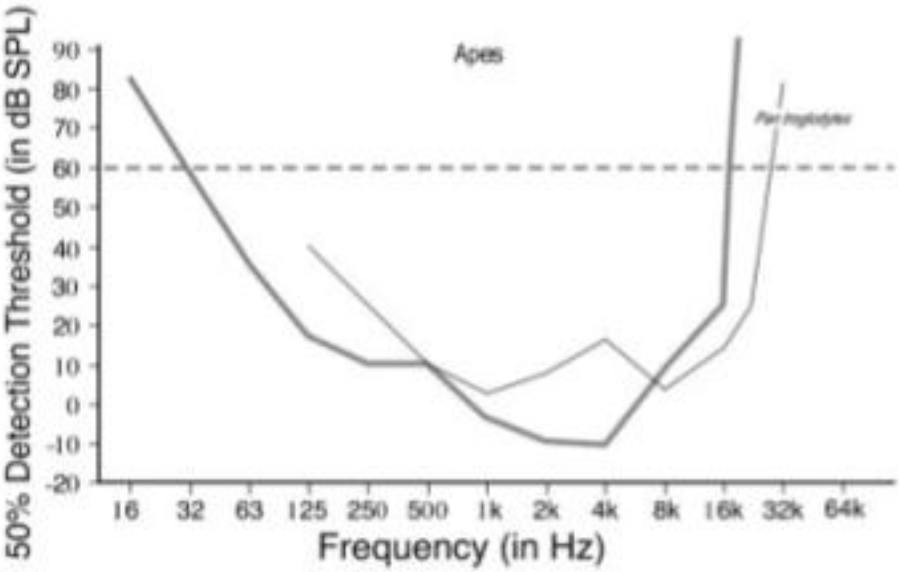

Fig. 7. Average audiogram for *Pan troglodytes* (Elder, 1934) and *Homo sapiens.* Figure from Heffner, 2004 reproduced with permission from John Wiley & Sons

Auditory structures in Neandertals

To date, no studies have published a functional analysis of Neandertal audition. However, several researchers have described various structures related to hearing with respect to taxonomic classification. For example, a recent study described and analyzed five new Neandertal ossicles from Qafzeh and Amud in southwest Asia (Quam and Rak, 2008). This study found clear differences between the ossicles in the Neandertal and *Homo sapiens* evolutionary lineages. Specifically, the researchers found that the Neandertal malleus differs from living humans in its larger dimensions and more open angle between the head and the manubrium (Quam and Rak, 2008). Similarly, the Neandertal incus has a straighter long process and more closed angle between processes than living humans (Quam and Rak, 2008). Although the anatomical variants considered in the study can be found in living humans, they occur at a higher frequency in Neandertals. The researchers therefore conclude that Neandertals consistently express only a portion of the modern human variation. Quam and Rak (2008) also compared the Neandertal ossicles to a fossil *H. sapiens* sample and found that the Neandertal malleus was clearly larger with respect to total malleus length, head length, and head width. However, they concede that these differences between Neandertals and fossil *H. sapiens* may be related to the generally larger body mass in Neandertals (Ruff et al., 1997). Lastly, the authors suggest that a combination of features in the malleus, incus, and stapes may indicate a slightly different positioning of either the tip of the incus long process or stapes footplate within the typmpanic cavity in the Neandertal lineage. The study makes no claims about the functional significance of such differences, but does suggest that the ossicles provide important information for assessing phylogenetic similarity.

A few studies have examined Neandertal inner ears, but they highlight the phylogenetic and functional impact of the vestibular system rather than the auditory system (Spoor et al., 2003, 2007). The semicircular canals have received particular attention because variation in their dimensions is associated with different head movements and locomotor behavior in mammals (e.g., Silcox et al., 2009; Spoor et al., 2007). Comparative analysis of the linear dimensions and angles of Neandertal semicircular canals has revealed morphological differences between Neandertals and modern *Homo sapiens*, which Spoor et al. (2003) interpret to reflect differences in locomotor behavior.

Spoor et al.'s (2003) comparative review of the Neandertal bony labyrinth also included descriptive measurements of the height and width of the basal turn of the cochlea and the radius of curvature of the basal turn (0.5[h + w]/2). Spoor et al. (2003) found that the size of the cochlear basal turn in Neandertals is not different from that of Holocene humans; whereas, it is slightly smaller than that of Upper Paleolithic and early anatomically modern humans. Across species, the size of cochlea correlates with body mass (Spoor and Zonneveld, 1998), so the researchers also took this relationship into account. When controlling for body mass, Holocene and Upper Paleolithic humans are not significantly different, but Upper Paleolithic humans have larger cochlear basal turns than Neandertals. Lastly, only the cochleae of modern humans are larger than predicted by body mass (Spoor et al., 2003).

Spoor and Zonneveld (1998) conducted a similar comparative review of the human bony labyrinth that included comparative data for extant primates, including gorillas and chimpanzees. In the study, the researchers found that after controlling for body mass, the cochlear basal turn of modern humans is larger than that of *Pan (troglodytes and paniscus),* which is, in turn, larger than that of *Gorilla* (Spoor and Zonneveld, 1998). Additionally, the cochlear basal turn of modern humans tends to be relatively wide (Spoor and Zonneveld, 1998).

Chapter IV

The Krapina Site

The Neandertal specimens in the current study derive from the archaeological site of Krapina. The town of Krapina is located in northern Croatia, about 40 kilometers northwest of Zagreb, the nation's capital. Just outside of Krapina lies Hušnjakovo (Hušnjak Hill), a rock shelter that is one of the most important late Pleistocene sites in Europe. This archaeological site, named after the nearby town, has yielded over 800 fragments of fossil hominids, a large collection of faunal remains, and over a thousand stone tools and débitage (Smith, 1976). The estimated number of individuals at Krapina ranges from 20 to more than 70 (Radovčić et al., 1988; Wolpoff, 1979). To date, Krapina consists of the largest number of Neandertal remains ever recovered from a single site.

Fig. 8. Dr. Dragutin Gorjanović-Kramberger. Photo from D. Frayer

Discovery and excavation of Krapina

The first Pleistocene finds at Krapina were made in 1895 when a local schoolteacher, Josip Rehorić, and a man named Kasimir Semenić discovered remains from extinct rhinoceros and bison in the rock shelter. Recognizing the antiquity of their finds, the men sent these fossils to Dr. Dragutin Gorjanović-Kramberger (Figure 8), the Director of the Geological-Paleontological Division of the National Museum in Zagreb (Radovčić, 1988).

Four years passed before Gorjanović was able to visit Krapina to investigate this site of Pleistocene animals. Upon his first visit, Gorjanović realized that Hušnjak Hill contained more than extinct rhinoceros and bison. Indeed, he discovered a sequence of hearths, a fragment of flint-like stone shaped for use, and a single human molar (Radovčić, 1988).

Elated with his discovery, Gorjanović drew up a detailed plan for excavating Krapina. He divided the entire sequence from lowest to highest into nine levels and a number of layers. All objects were excavated by layer and marked with a number that indicated their provenience. This meticulous approach to excavation was unusual for the time and is often cited as the first modern excavation of human fossils (Radovčić, 1988). Gorjanović reported the discoveries of his first season in record time after completing the excavation. Within two years, he had published both a general description of the site and a report of the first hominid remains: five teeth, a temporal bone, and a maxilla (Smith, 1976).

Excavations at Krapina resumed in the summer of 1900. This field season's yield was not as abundant as the previous year, but Gorjanović still recovered a number of hominid and faunal remains (Smith, 1976). Having fallen ill with tuberculosis, Gorjanović placed the direction of the 1902 field season under Stjepan Osterman, his primary assistant. This season yielded a juvenile mandible, thirty-two hominid teeth, and a large skeletal series of *Rhinoceros mercki* (Gorjanović, 1906, cited in Smith, 1976). The 1903 excavation, again under the direction of Gorjanović, was mainly concentrated around the edges of the Hušnjakovo rock shelter and elsewhere on the hill. Still, the limited excavations in the shelter itself yielded a few hominid remains (Gorjanović, 1906, cited in Smith, 1976).

In 1905 Gorjanović embarked on the largest scale excavation attempted at Krapina. In this year alone he discovered more than 200 skeletal fragments and thirty-eight isolated teeth

(Radovčić, 1988). Most of the Neandertal collection was excavated at this time, including the more familiar Krapina specimens. At the end of the excavation period from 1899 to 1905, Gorjanović had collected over 800 hominid fragments, more than 1000 flint artifacts and 3000 remnants of animal bones (Radovčić, 1988).

Though he published data on his finds during the six-year excavation period, Gorjanović's most thorough and exhaustive work was his 1906 monograph. Entitled "Der Diluviale Mensch von Krapina in Kroatien" ("Diluvial man from Krapina"), this monograph was published as a contribution to Otto Walkhoff's "Studien über die Entwickelungsemchanik des Primatenskelettes" (Smith, 1976). The monograph contains a description of the geologic background of the site and a brief discussion of the faunal and archaeological remains. However, the publication is most notable for its detailed descriptions of the Krapina hominid remains. The publication contained the most extensive work on fossil man at the time and is still frequently cited in paleoanthropolgy textbooks (Radovčić, 1988).

Gorjanović continued to publish on the Krapina remains until 1929. In fact, he published an additional 35 scientific papers, including one additional monograph, in the 23 years following the publication of "Diluvial man from Krapina" (Smith, 1976). He died in 1936 at the age of eighty, but his contribution to the fields of paleontology and paleoanthropology established him as one of the great scientists of his day.

Stratigraphy and chronology

As mentioned above, the stratigraphic levels at Krapina were well described by Gorjanović. The profile, spanning 9 meters, has well-defined cultural layers that Gorjanović classified by predominant fauna. The lowest layers (1 and 2) are river gravels dominated by beaver remains (*Castor fiber).* Layers 3 and 4, abundant with hominids, are termed the *Homo* *sapiens* zone. Above the *Homo sapiens* zone, Merck's rhinoceros (*Stephanorhino kirchbergensis*) dominate layers 5-7, although cave bears (*Ursus spelalus)* also make an appearance at the top of this zone. Rhinos are present throughout the entire sequence from layers 2 through 7; thus, the *Homo sapiens* zone may actually be a subset within the rhino zone (Caspari & Radovčić, 2006).

Although the majority of Krapina hominid remains derive from the *Homo sapiens* zone, there are accumulations of Neandertal fossils later in the sequence in layer 8. This may suggest two occupations of the site, but the presence of hearths, lithics, and charred bones throughout the sequence indicates continuous occupation (Caspari & Radovčić, 2006). The high frequency of lithics and hominid remains in the *Homo sapiens* zone may represent a different or more intensive use of the site at that time, rather than a distinct occupation (Caspari & Radovčić, 2006). Furthermore, electron spin resonance (ESR) and uranium- (U) series dates derived from the top and bottom of the sequence are both about 130,000 BP, suggesting a short time period for the entire sequence (Rink et al., 1995). Interestingly, Gorjanović came to a similar conclusion based on the rate of sedimentation at the site. He interpreted the entire sequence from Layer 1 to 9 to represent no more than about 8,000 years (Gorjanović, 1913, cited in Caspari & Radovčić, 2006).

The chronology of the *Homo sapiens* zone itself is also consistent with Gorjanović's 1913 interpretation. Based on the nature of the total faunal sample and the geological context of the site, Gorjanović contended that Krapina dated to the last interglacial, the Riss-Würm (Gorjanović, 1913, cited in Caspari & Radovčić). Although some authors later suggested the Krapina hominids dated to interstadials within the Würm glaciation (e.g. Brace, 1964; Malez, 1978), modern technology ultimately confirmed Gorjanović's original interpretation. Indeed, ESR dates from rhino teeth from levels bracketing the *Homo sapiens* zone suggest an age of 120,000 to 140,000 years BP, a date consistent with the beginning of the last interglacial (Rink et al., 1995).

Chapter V

The Current Study

The purpose of the current study is to examine the cochlear volume of nine Krapina Neandertals utilizing 3D reconstructions generated from ultra high-resolution computed tomography (uhrCT) scans. The Neandertal cochleae are compared to chimpanzee, gorilla, and modern human samples. These analyses offer information about the cochlear variation of Krapina Neandertals and are the first to compare cochlear volumes of Neandertals and modern humans. Although Spoor et al. (2003) measured linear dimensions of the cochlear basal turn, labyrinth volume has yet to be studied in Neandertals. In light of Kirk and Gosselin-Ildari's (2009) recent description of the functional relationship between cochlear volume and hearing abilities in primates, the cochlear volume of Neandertals offers insight into their hearing abilities relative to modern humans.

Based on the literature (e.g. Spoor and Zonneveld, 1998; Spoor et al., 2003; Kirk and Gosselin-Ildari, 2009), classification of species in ascending absolute cochlear labyrinth volume is hypothesized to trend in the following order: chimpanzee, gorilla, Neandertal, modern human. Neandertal absolute cochlear volume is hypothesized to be statistically the same as that of modern humans, and statistically larger than that of gorillas and chimpanzees. When taking body mass into account, it is hypothesized that relative cochlear labyrinth volume would trend in the following ascending order: gorilla, Neandertal, modern human, chimpanzee. This follows from the negative allometric relationship between cochlear volume and body mass in primates (Kirk and Gosselin-Ildari, 2009) which means that the ratio of cochlear volume to body mass (scaled volume) increases as body mass decreases. Following Spoor et al.'s (2003) findings regarding the size of the cochlear basal turn, only the cochlear volume of modern humans is hypothesized to be larger than predicted by body mass.

Materials and methods

Specimens and CT scanning

The study sample consists of nine Neandertal (*Homo sapiens neandertalensis*) temporal bones from Krapina (Table 1). The nine specimens were selected for CT scanning by Dr. Radovčić of the Croatian Natural History Museum because of the likelihood that they had preserved inner ear structures. Although Krapina 3 (Cranium C) has an associated temporal bone, it was unable to be transported for CT scanning. Most of the sample is comprised of isolated temporal bones or petrosals, but one specimen, K39.4, is associated with Krapina 1 (Cranium A). Both mature (n=8) and immature (n=1) specimens are represented, but age differences will not be reflected in cochlear volume because the bony labyrinth reaches adult size between the 17th and 19th weeks of gestation (Jeffery and Spoor, 2004). Ultra high-resolution computed tomography scans were acquired for each temporal bone from the Vienna micro-CT lab (http://micro-ct.at/) at the University of Vienna, Austria. The Krapina temporals were all reconstructed to 25 μm^3 isotropic voxels, meaning the pixel dimensions and the slice thicknesses for all scans were set to exactly 0.025 mm. 1440 slices were acquired for each scan. Due to the fragmentary nature of the sample, the specimens were scanned in variable orientations that do not conform to standard anatomical planes.

Table 1.
Krapina Neandertal sample with inner ear preserved

Fossil	Side	Developmental Age	Temporal bone preservation
K38.1	R	Adult	From the sphenosquamosal suture to the asterionic notch with about 2/3 of the petrosal
K38.12	R	Adult	Includes mastoid process, the external auditory meatus, and most of the petrosal
K38.13	R	Adult	Includes most of the petrosal and mastoid
K39.13	L	Adult	Posterior part, includes the petrosal
K39.1	L	Adult	Almost complete temporal
K39.4_K1	L	Juvenile	Part of Krapina 1 (Cranium A), complete left temporal
K39.8	R	Adult	Part of Krapina 38.21 , includes most of thepetrosal and mastoid
K39.18	L	Adult	Most of the petrosal
K39.20	L	Adult	Lateral part of petrosal, possibly the antimere to K38.13

Information from Radovčić et al., 1988

Abbreviations: K, Krapina

The comparative sample consists of ten modern humans (*Homo sapiens sapiens*), five chimpanzees (*Pan troglodytes*), and five gorillas (*Gorilla gorilla*) (see Table 2). The modern humans are a sample of Oneota from Norris Farms in Illinois, dating to ~1300 A.D. (Milner and Smith, 1990) Specimens included in the sample were adults, based on 3rd molar eruption. The modern human scans have pixel dimensions (x/y axes) ranging from 0.0615 to 0.0781 mm and slice thicknesses (z axis) ranging from 0.0696 to 0.0879 mm. The chimpanzee and gorilla samples are adult, wild-shot specimens from the American Natural History Museum and the National Museum of Natural History. Sex of each specimen was identified using standard osteological techniques. The chimpanzee scans have pixel dimensions ranging from 0.0635 to 0.0750 mm with slice thicknesses ranging from 0.0707 to 0.0885 mm. The gorilla sample has pixel dimensions ranging from 0.0781 to 0.0830 mm with slice thicknesses ranging from 0.0879 to 0.0938 mm. All three comparative samples were scanned at the Pennsylvania State University Center for Quantitative X-ray Imaging (www.cqi.psu.edu). Although the specimens were not scanned in perfectly identical orientations, the comparative sample scans largely conform to a series of slices running through the rostro-caudal (transverse) axis of the petrosal.

Table 2.
Comparative sample composition

Modern Humans **n=10**	**x,y (mm)**	**z (mm)**
Norris Farms 820227 (f)	0.0781	0.0879
Norris Farms 820648 (m)	0.0781	0.0879
Norris Farms 820696 (f)	0.0781	0.0879
Norris Farms 820726 (m)	0.0781	0.0879
Norris Farms 820735 (m)	0.0781	0.0879
Norris Farms 821110 (f)	0.0781	0.0879
Norris Farms 821129 (f)	0.0615	0.0696
Norris Farms 821205 (f)	0.0615	0.0696
Norris Farms 821211 (f)	0.0615	0.0696
Norris Farms 821221 (m)	0.0781	0.0879
Chimpanzees **n=5**	**x,y (mm)**	**z (mm)**
AMNH 54330 (m)	0.0732	0.0830
AMNH 90191 (f)	0.0750	0.0885
AMNH 167343 (f)	0.0635	0.0707
AMNH 167344 (m)	0.0750	0.0844
AMNH 167346 (m)	0.0664	0.0740
Gorillas **n=5**	**x,y (mm)**	**z (mm)**
AMNH 167330 (f)	0.0830	0.0938
AMNH 167337 (f)	0.0781	0.0879
NMNH 176210 (m)	0.0820	0.0917
NMNH 176216 (m)	0.0820	0.0917
NMNH 176220 (m)	0.0820	0.0917

Abbreviations: AMNH, American Museum of Natural History;
NMNH, National Museum of Natural History; m, male; f, female

Delimitation of the cochlea

Following Kirk and Gosselin-Ildari (2009), all images in the scan sequence that did not include the cochlea were discarded in order to facilitate distinguishing the cochlear labyrinth from the vestibule. The remaining images were cropped using Amira 5.3.3 software (www.amira.com) to a box that tightly enclosed the cochlea. The base of the cochlear labyrinth is identified using the bony structures associated with the scala media and scala tympani. The beginning of the scala media, or membranous cochlear duct, can be identified as the first appearance of the "basilar gap." This term refers to the space between the primary and secondary osseous spiral laminae where the basilar membrane attaches (Kirk and Gosselin-Ildari, 2009). Similarly, the beginning of the scala tympani can be identified as the first appearance of the round window. The beginning of the scala vestibuli, on the other hand, has no bony markers to indicate its

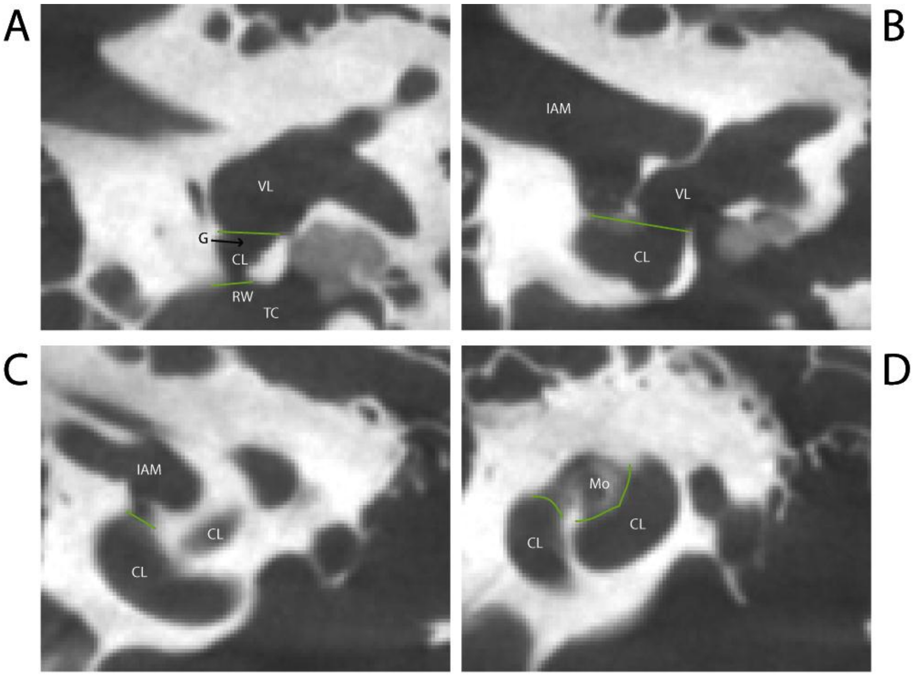

Fig. 9. Successive CT slices from a chimp petrosal depicting the bounding lines (shown in green) drawn around the cochlear labyrinth. In slice A, two bounding lines are necessary: one to separate the cochlear and vestibular labyrinths and one to close the round window. In slice B, the bounding line separates the cochlear labyrinth from the vestibule and reinforces the boundary between the cochlear labyrinth and internal acoustic meatus. In slices C and D, the bounding line reinforces the boundary between the cochlear labyrinth and the internal acoustic meatus and modiolus, respectively. Abbreviations: CL, cochlear labyrinth; G, basilar gap; IAM, internal acoustic meatus; Mo, modiolus; RW, bounding line closing off the round window; TC, tympanic cavity; VL, vestibular labyrinth.

presence. Thus, boundaries of the cochlea spanned from the first appearance of the basilar gap to the last slice in which the cochlear apex was visible.

For the gorilla, chimpanzee, and modern human specimens, which were all scanned in similar orientations, the first slice of the cochlear sequence in the x/y plane was the boundary between the vestibule and the cochlea, identified by the first appearance of the basilar gap or round window (Figure 9). The Neandertal specimens, on the other hand, were scanned in different orientations and the first image containing the cochlea in the x/y plane did not necessarily show the base of the cochlea. Thus, although the basilar gap and round window aided in cochlear delimitation, the slices with these structures were not always the first slices in the

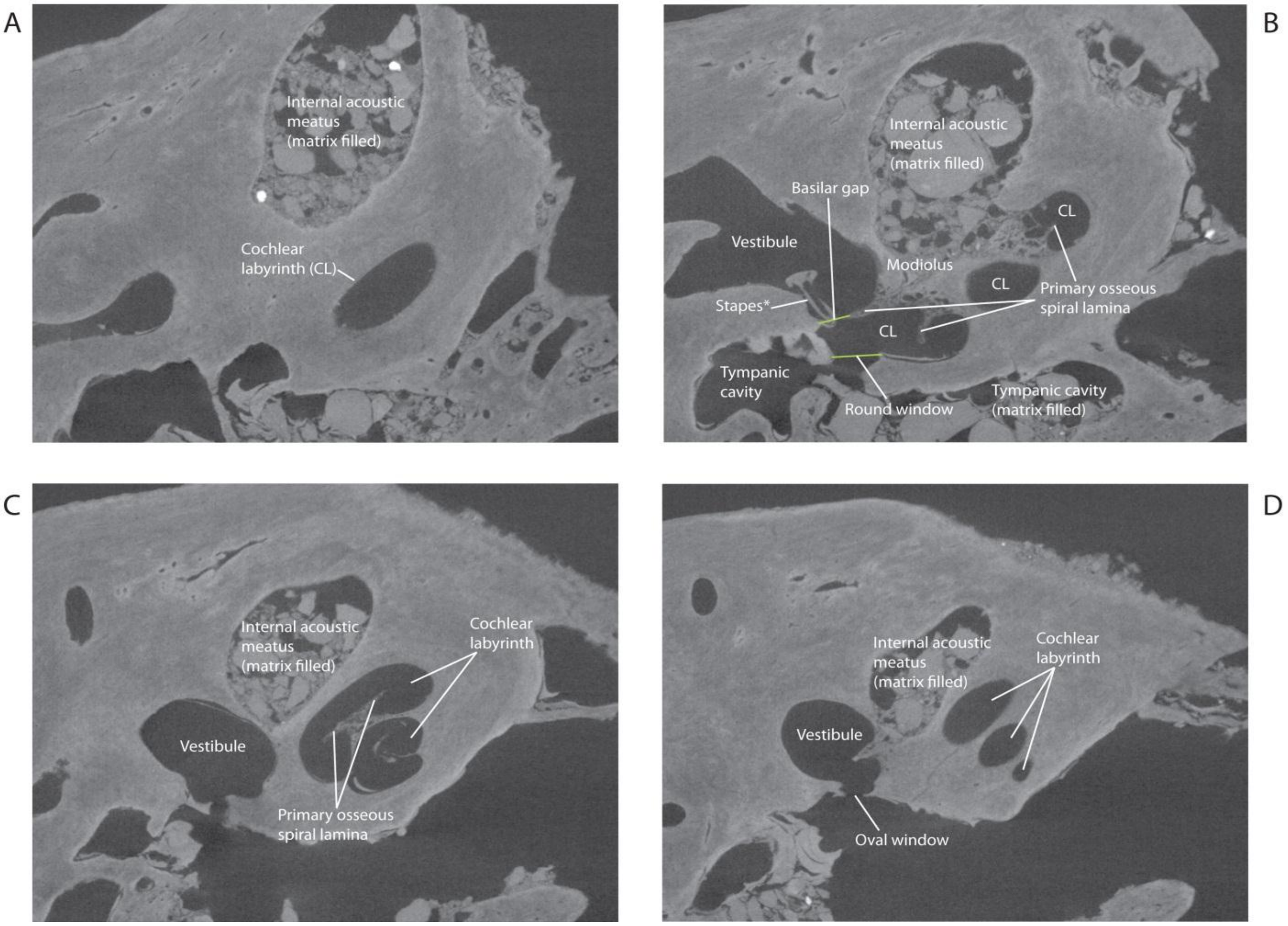

Fig 10. Successive CT slices through the petrosal of a Neandertal (K39.13) illustrating bounding lines (shown in green) and various anatomical structures. *Note that the stapes is not in anatomical position, and has fallen through the oval window into the vestibule.

cochlear sequence. See Figure 10 for an illustration of successive slices through a Neandertal petrosal in the x/y dimension.

Segmentation, thresholding, and 3D reconstruction

Segmentation is the process of highlighting a particular structure of interest from each image in the scan sequence. The segmented areas are ultimately combined to create the 3D reconstruction of the desired anatomical structure, in this case, the cochlea. For this study, cropped image sequences were imported into Amira and segmented in the image segmentation editor module, using either the magic wand or paintbrush tools.

Following Kirk and Gosselin-Ildari (2009), several series of bounding lines were drawn with the line tool in Amira to separate the cochlear labyrinth from the vestibule, tympanic cavity, modiolus, and internal acoustic meatus (Kirk and Gosselin-Ildari, 2009; see Figures 9 and 10 for illustrations of the bounding lines). When closing off the cochlea from the vestibule, a bounding line was drawn from the primary osseous spiral lamina to the nearest edge of the oval window. When the junction of the vestibule and cochlea began to “pinch”, the bounding line was moved to the narrowest point of the confluence between the two structures. When separating the cochlea from the tympanic cavity, a bounding line was drawn between the two bony edges of the round window in any slice where the hole was open. Additional bounding lines were drawn as necessary to separate the cochlear labyrinth from the modiolus and internal acoustic meatus.

The threshold between the air-filled cochlear labyrinth and the bone surrounding it was estimated using the half maximum height (HMH) technique (Spoor and Zonneveld, 1995). Due to limited spatial resolution, CT numbers (grayscale values assigned to each pixel) change gradually at the boundary of a structure. The air-bone interface is estimated to be halfway between the 2 CT numbers on either side of the structure (Spoor and Zonneveld, 1995). Thus, the

HMH method averages the highest and lowest CT numbers on either side of an interface to yield a threshold value that estimates the true boundary of the cochlea. This threshold value determines which pixels are included and excluded when segmenting. Because the cochlear labyrinth is surrounded by dense cortical bone, but winds around the porous modiolus, one HMH value is not sufficient to accurately delineate the cochlea throughout the entire image sequence. HMH values calculated at the outer edge of the cochlear labyrinth overestimate the boundaries of the cochlea by including portions of the bone around the modiolus and the spiral osseous lamina. HMH values calculated at the inner edge of the cochlear labyrinth, however, underestimate the boundaries of the cochlea and often fail to include portions of the canal lumen. Thus, two separate HMH thresholds for each scan sequence were calculated with the plot profile function in Image J (http://rsbweb.nih.gov/ij) (Kirk and Gosselin-Ildari, 2009). The low threshold was the HMH value calculated at the inner edge of the cochlear labyrinth, at the boundary between the cochlear lumen and the osseous spiral lamina. Another HMH value was calculated at the outer edge of the cochlear labyrinth, or the boundary between the cochlear lumen and the dense petrous bone surrounding the labyrinth. This second HMH value is extremely high and includes the spiral laminae and modiolus in selections of the cochlea. The second HMH value was averaged with the low threshold HMH value to produce the high threshold value.

Two separate cochlear labyrinth volumes were calculated in Amira for the chimpanzee and gorilla samples (Kirk and Gosselin-Ildari, 2009). For the first volume calculation, the threshold settings for the magic wand tool in the image segmentation editor were set to the low threshold values. Bounding lines were applied to each image in the manner described above, and the air-filled space of cochlear labyrinth was manually selected in each slice using the magic wand tool. After segmenting the entire cochlear sequence, the surface gen function in Amira was used to create a 3D model of the selected area. Volumetric measurements were taken from the resulting 3D reconstruction using the volumetric measurement function. Because this 3D model was created with the low threshold, this yielded a minimum cochlear labyrinth volume that likely underestimates actual cochlear volume. The same process was repeated with the high threshold value to create the maximum cochlear labyrinth volume measurement, which likely overestimates actual cochlear volume. The final estimate of cochlear volume was calculated by averaging the minimum and maximum cochlear volume measurements.

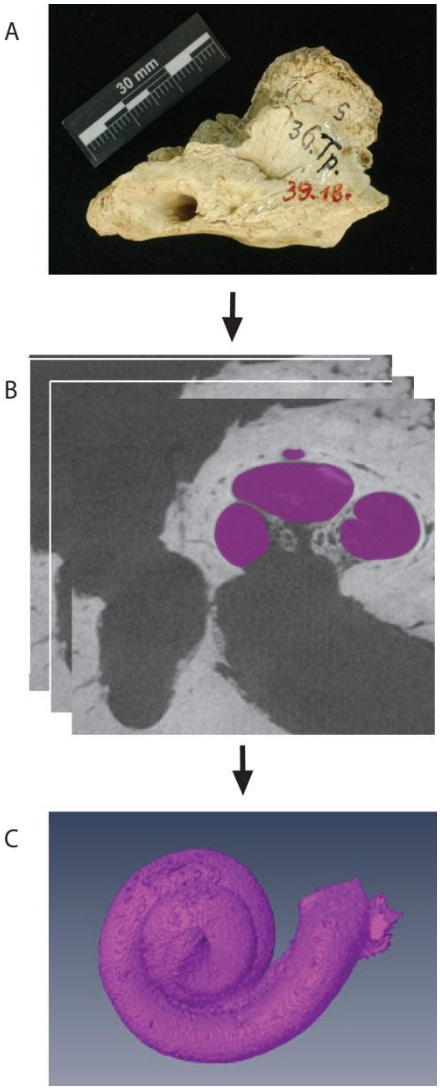

Fig 11. Schematic representation of segmenting and 3D cochlear reconstruction. Box A is a lateral view of the osteological specimen K39.18. Box B illustrates the process of segmenting the cochlear labyrinth with a high threshold color in the µCT scans, and Box C shows the final 3D reconstruction of the cochlea.

The bony labyrinths of the modern human and Neandertal specimens were often filled with matrix that was nearly identical to the density of the surrounding bone. Consequently, the semi-automated method using the magic wand tool was inappropriate because it failed to include large portions of the cochlea in the images that included matrix. Instead, the half maximum height method was used to assist in identifying the air-bone (often matrix-bone) boundary, but segmentation for the archaeological specimens frequently relied on manual highlighting of the cochlear labyrinth with the paintbrush tool. To facilitate accurate identification of anatomical structures, image segmentation with this manual method was carried out not only in the original x/y plane, but also in the z/x and y/z planes. Following segmentation with the manual method, the Surface Gen function in Amira was used to create a 3D model of each modern human and Neandertal cochlea. A single volumetric measurement was taken from each 3D reconstruction using the volumetric measurement function. Figure 11 shows a schematic illustration of segmenting and 3D cochlear reconstruction for one of the Neandertal specimens.

Error and validation

To provide a validity check of the manual segmenting method, the chimpanzee and gorilla samples were segmented with the manual method, in addition to the semi-automatic magic wand method. The cochlear volumes obtained with the manual method were less than 5% different from the volumes obtained using the semi-automated method (see Appendix A). Additionally, three of the modern human scans were re-segmented months after the original manual segmentation to check the reliability of the method (see Appendix B). Lastly, the chimpanzee and modern human cochlear labyrinth volumes derived from the manual segmenting method are comparable to the volumes presented in Kirk and Gosselin-Ilardi (2009).

Statistical analyses

Following validation of the manual segmenting method, statistical analyses of manual cochlear volumes were performed using PASW Statistics 18 software (www.spss.com). When several volume measurements were collected, the average of the values was used in the analysis. Mean cochlear volumes of the four samples were compared using Kruskal-Wallis H-test and Mann-Whitney U-tests, which are the nonparametric equivalents of one-way ANOVA and independent t-tests, respectively (Samuels and Witmer, 2003). Because cochlea size scales with body mass (Spoor and Zonneveld, 1998), statistical tests were performed before and after scaling each individual’s cochlear volume by its species’ body mass. For the scaled data analysis, both cochlear labyrinth volume and body mass were $\log_{10}$ transformed to account for the nonlinear, allometric relationship between cochlear volume and body mass. Estimated body masses follow Smith and Jungers (1997) for chimpanzees, gorillas, and modern humans, and Ruff et al. (1997) for Neandertals. Since the sex was known for chimpanzees, gorillas and moderns humans, it was possible to use sex-specific body mass estimates for these samples.

Lastly, Pearson correlation and linear regression analyses were used to examine the relationship between cochlear labyrinth volume and body mass. The bivariate plot of $\log_{10}$ cochlear volume by $\log_{10}$ body mass includes data on 31 primate species from Kirk & Gosselin-Ildari (2009) in addition to the current data for gorillas, chimpanzees, modern humans, and Neandertals. For the two species where both Kirk & Gosselin-Ildari (2009) and the current study have data (*Pan troglodytes* and *Homo sapiens sapiens*), the current data were used. For the regression analyses, mean cochlear volume and mean body mass estimates were used for each group. Because body mass correlates with cochlear volume across species (Kirk and Gosselin-Ildari, 2009), rather than within species, a single body mass estimate was used for each group even in the presence of sexual dimorphism (i.e. gorillas). However, where sex of the specimens is known (gorillas, chimps, and moderns), the species body mass estimate is a weighted average based on the sex composition of the sample. For example, the body mass estimate for modern human males is 62.2 kg and for females is 54.43 kg (Smith & Jungers, 1997). Because the current sample is comprised of 4 males and 6 females, the mean body mass for moderns humans used in the regression was calculated as [4(62.2) + 6(54.43)]/10, which equals 57.54 kg.

Both ordinary least squares (OLS) regression and reduced major axis (RMA) regression were calculated. OLS regression is the standard method to fit a trend line and is appropriate to use when predicting values of the y-axis (dependent variables) from values of x-axis (independent variables) (Smith, 1994). RMA regression, an alternative to OLS regression, is appropriate to use when examining the scaling relationship between variables (Warton et al., 2006) or when error is present in measurement of both the x-axis and y-axis variables (Hofman et al., 1986). OLS is often described as requiring the assumption that X is measured without error while RMA regression incorporates the assumption that X is measured with error (Smith, 2009). For the current study, measurement error is associated with the x-axis variable (body mass estimation), which indicates that RMA regression may be the appropriate analysis. However, measurement error in X as the sole criterion for selecting RMA regression rather than OLS regression has been questioned (Smith, 2009). Additionally, OLS regression is generally considered to be the more appropriate analysis when the regression line is used for prediction (Smith, 2009). Thus, both OLS and RMA regression analyses are presented in the current study. RMA regression is used to examine the scaling relationship between cochlear volume and body mass, and both OLS and RMA regression are considered when comparing each group’s observed mean cochlear volume to the mean cochlear volume predicted by the species’ body mass.

Chapter VI

Results

Qualitative analysis

Three dimensional (3D) reconstructions of the modern human and Neandertal archaeological specimens yielded cochleae that were generally intact, attesting to the fact that the cochlea is often the best preserved region of the auditory system in fossils (Coleman et al., 2010). Some of the Neandertal specimens were poorly preserved near the basal region of the cochlea, but the extent of taphonomic damage did not significantly affect the general shape or volume of the 3D reconstruction. Given their geologic age, the Neandertal specimens are remarkably well-preserved. For example, figure 12 shows that 3D reconstructions of the inner ear structures of one of the Neandertal specimens (K39.13) are well-preserved and free from distortion.

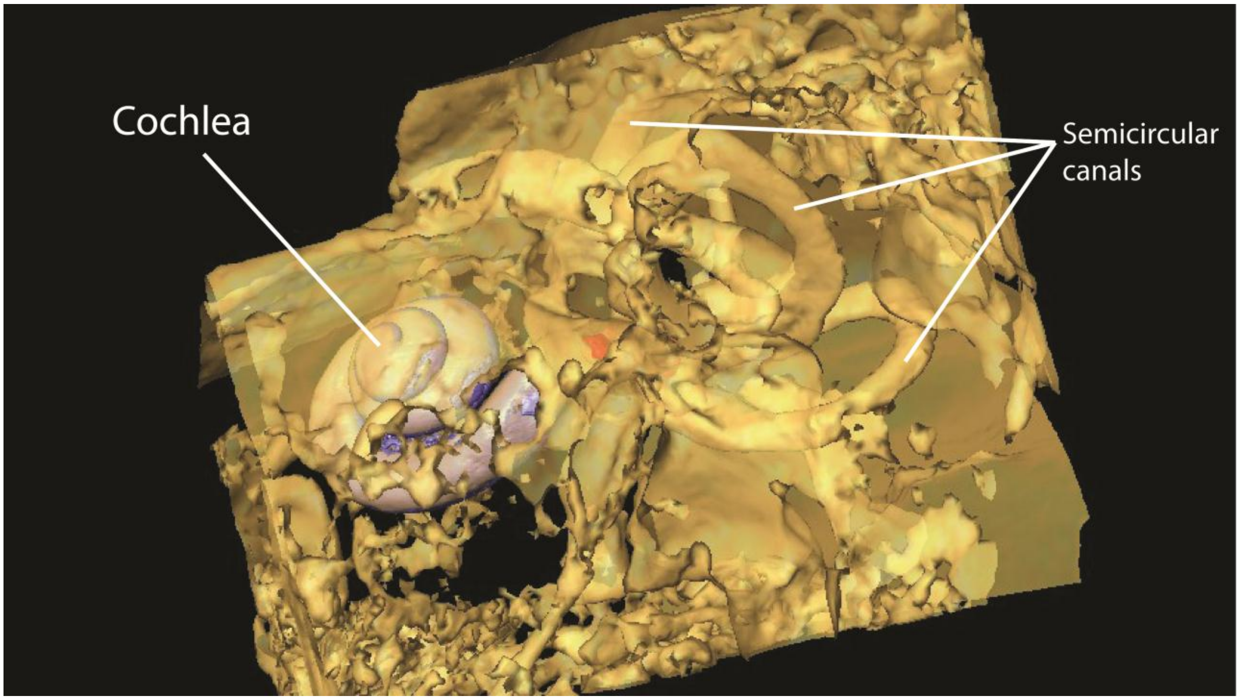

Fig. 12. The inner ear structures of Krapina 39.13. The cochlear labyrinth is shown in purple and the semicircular canals are visible to the right of the cochlea. Reconstruction is not in anatomical position.

Overall, the gorilla and chimpanzee museum specimens, as well as the modern human and Neandertal archaeological specimens, exhibited a level of preservation that allows for accurate estimates of cochlear shape and volume. Figure 13 shows representative 3D cochlear reconstructions for each of the four groups studied. As shown in the figure, the gross morphology of the cochlea for the four different groups is similar. The number of cochlear turns for each specimen was visually estimated by manually tracing the outer circumference of the 3D reconstruction from the distal edge of the round window to the approximate location of the helicotrema (Table 3). The number of cochlear turns for gorillas ranged from 2.75 to 3 turns, with most specimens exhibiting 2.75 turns. Chimpanzees had the same range (2.75-3 turns), but most specimens exhibited 3 full cochlear turns. The range of cochlear turns for modern humans was 2 to 2.5, with a majority of the specimens having 2.5 spiral turns. The number of cochlear turns for Neandertals ranged from 2.5 to 3 turns. Though slightly more variable than the moderns humans, most (5/9) of the Neandertal specimens had 2.5 cochlear turns. Considering the large variation of cochlear turns among species, and even within a single species (see Ni et al., 2010), the implications of the number of cochlear turns remain unclear.

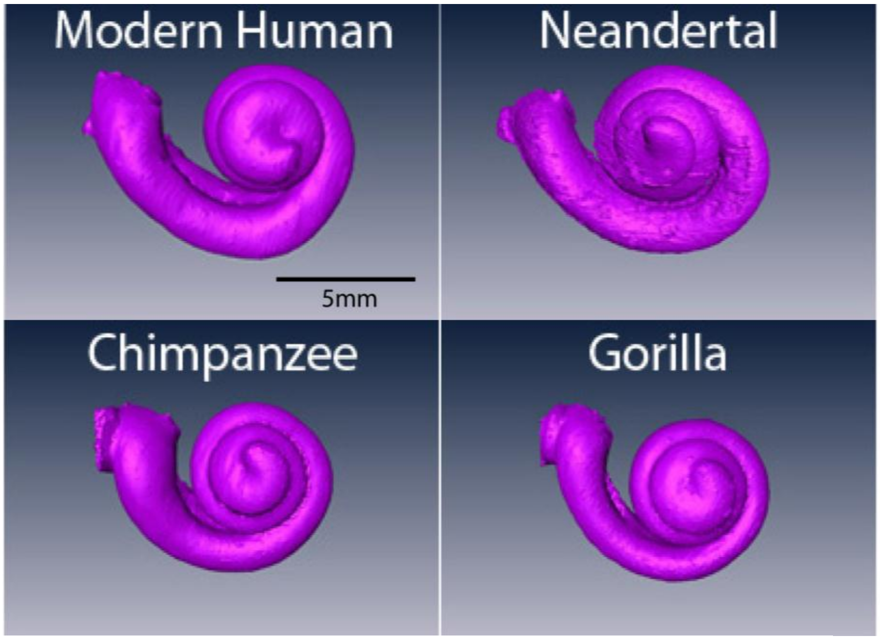

Fig. 13. This figure illustrates selected 3D reconstructions of cochlear labyrinths. The cochleae are oriented so that the round window faces left and the scale is the same for each picture.

Table 3.
Number of cochlear turns

	No. of specimen	**No. of turns**	**Percent of Sample**
Gorillas	4	2.75	80
n=5	1	3	20
Chimps	1	2.75	20
n=5	4	3	80
Modern Humans	1	2	10
n=10	1	2.25	10
	8	2.5	80
Neandertals	5	2.5	56
n=9	2	2.75	22
	2	3	22

Quantitative Analysis

<u>Descriptive statistics</u>

Mean absolute cochlear volume, standard deviations, coefficients of variation, minimum, maximum, and range for each species can be found in Table 4. Figure 14 presents an illustration of each Neandertal cochlear labyrinth reconstruction as well as the associated cochlear volume (mm^3). Classification of the species in ascending mean absolute cochlear labyrinth volume trends in the following order: chimpanzee, gorilla, Neandertal, modern human.

Table 4.
Absolute cochlear labyrinth volume

	Mean Cochlear Volume (mm^3)	Standard Deviation (mm^3)	Coefficient of Variation	Minimum (mm^3)	Maximum (mm^3)	Range (mm^3)
Gorillas (n=5)	63.40	6.14	0.10	55.73	72.32	16.59
Chimpanzees (n=5)	55.98	9.27	0.17	47.56	69.49	21.93
Modern Humans (n=10)	80.01	7.86	0.10	66.59	89.88	23.29
Neandertals (n=9)	77.40	6.32	0.08	65.14	85.65	20.52

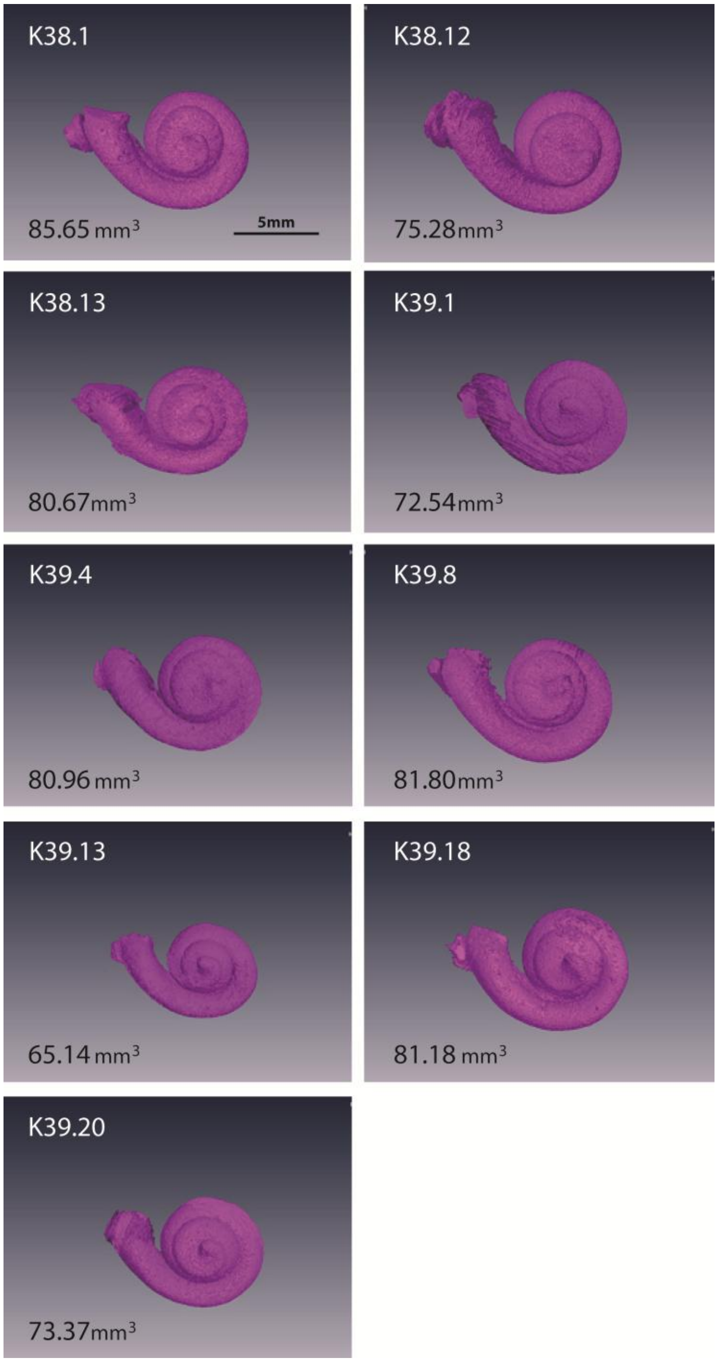

Fig. 14. 3D reconstruction of each Neandertal cochlear labyrinth. Specimen number is found in the upper left corner of each picture and cochlear volume is found in the lower left corner. The scale is the same for each cochlea.

Examination of the coefficients of variation (standard deviation divided by the mean) indicate the Neandertal sample shows the least variation in cochlear labyrinth volume (0.08), while modern humans and gorillas have the same amount of variation (0.10), and the chimpanzee sample shows the most variation (0.17).

<u>Nonparametric analyses</u>

Absolute cochlear volume

A Kruskal-Wallis H-test demonstrates a significant difference between the mean absolute cochlear volumes of the different groups (p = .001), indicating at least one significant pairwise difference between groups. Pairwise Mann-Whitney U-tests (Table 4) show that Neandertal absolute cochlear volume is statistically no different from modern humans (p = 0.414), but significantly larger than gorillas (p = 0.004) and chimpanzees (p

= 0.004), whose absolute cochlear volumes are not statistically different from each other (*p* = 0.175). While not surprising, it is nevertheless important to note that Neandertals are aligned closely with modern humans and significantly larger than large-bodied and small-bodied apes.

Scaled cochlear volume

Since other studies indicate cochlear volume scales to body size (Kirk and Gosselin-Ildari, 2009; Armstrong et al., 2011) cochlear labyrinth volume scaled relative to body mass ($\log_{10}$ cochlear volume/ $\log_{10}$ body mass) was also analyzed using nonparametric statistical analyses (Table 5). A Kruskal-Wallis H-test shows a significant difference among the mean scaled cochlear volumes of the different groups ($p = 0.001$). Mann-Whitney U-tests (Table 5) show that Neandertal scaled cochlear volume is statistically smaller than that of modern humans ($p = 0.001$) and chimpanzees ($p = 0.003$), and statistically larger than that of gorillas ($p = 0.003$). Only modern human and chimpanzee scaled cochlear volumes were similar to each other ($p = 0.0142$).

Table 5.
p-values for Mann-Whitney U-tests

Group	Mean Absolute Cochlear Volume (mm^3)	Body Mass Estimate (kg)		Mean Scaled Cochlear Volume*
		Male	**Female**	
Gorillas (n=5; 3 male, 2 female)	63.4	170.4	71.5	0.871
Chimpanzees (n=5; 3 male, 2 female)	55.98	42.7	33.7	1.097
Modern Humans (n=10; 4 male, 6 female)	80.01	62.2	54.43	1.081
Neandertals (n=9; sex unknown)	77.4	76	76	1.003

Pairwise Comparison	p-value	p-value
Neandertal Modern Human	0.414	**0.001**
Neandertal Chimpanzee	**0.004**	**0.003**
Neandertal Gorilla	**0.004**	**0.003**
Modern Human Chimpanzee	**0.003**	0.142
Modern Human Gorilla	**0.005**	**0.002**
Gorilla Chimpanzee	0.175	**0.009**

Mann-Whitney U-tests that reached statistical significance ($p \leq 0.05$) are shown in bold font

* scaled volume = log10 Cochlear Volume/ log10 Body Mass

body mass estimates for gorillas, chimps, and moderns follow Smith & Jungers (1997) specific

body mass estimate for Neandertals follows Ruff et al. (1997)

Linear regression

In addition to nonparametric analyses, the current data were analyzed with respect to a linear regression of cochlear volume on body mass that includes primate data from Kirk & Gosselin-Ildari (2009). Cochlear labyrinth volume is significantly positively correlated with body mass (r = 0.924; *p* = 0.001). Figure 15 presents a bivariate plot of log10 cochlear volume

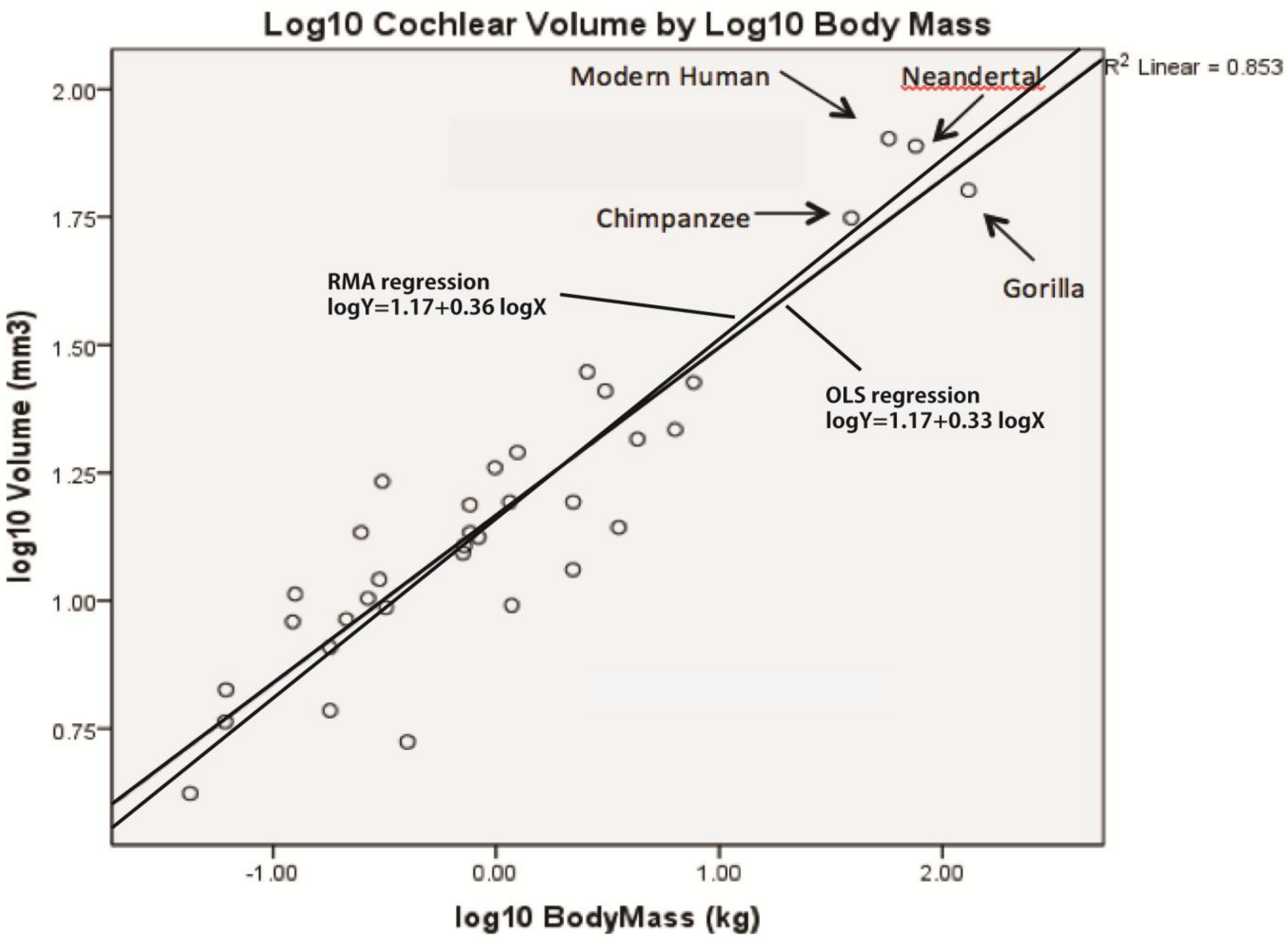

Fig. 15. Bivariate plot of log10 cochlear volume (in mm^3) by log10 body mass (in kg) including primate data from Kirk and Gosselin-Ildari (2009), and the four current groups.

humans, however, were both larger than predicted by body mass and fell outside of the 95% confidence interval. Using RMA regression, the observed cochlear labyrinth volumes for gorillas trended smaller than predicted by body mass, and chimpanzees and Neandertals trended larger than predicted by body mass. Still, the observed volumes were within the 95% confidence interval of the predicted value for all three groups. With RMA regression, only modern human cochlear labyrinth volume was larger than predicted by body mass.

Table 6.
Values of mean cochlear volume (mm3) predicted by body mass (kg)

Ordinary Least Squares (OLS) Regression

	Body Mass	Predicted Cochlear Volume	95% Confidence Lower Limit	95% Confidence Upper Limit	Observed Cochlear Volume
Gorillas	130.84	72.81	56.57	93.72	63.40
Chimpanzees	39.1	48.96	40.10	59.79	55.98
Modern Humans	57.54	55.59	44.78	69.01	**80.01**
Neandertals	76	60.91	48.47	76.54	**77.40**

Reduced Major Axis (RMA) regression

	Body Mass	Predicted Cochlear Volume	95% Confidence Lower Limit	95% Confidence Upper Limit	Observed Cochlear Volume
Gorillas	130.84	83.18	63.1	109.65	63.4
Chimpanzees	39.1	53.70	42.66	67.61	55.98
Modern Humans	57.54	61.66	47.87	79.43	**80.01**
Neandertals	76	69.18	52.48	89.13	77.4

body mass estimates for gorillas, chimps, and moderns follow Smith & Jungers (1997) and are the sex-specific averages of the current sample

body mass estimate for Neandertals follows Ruff et al. (1997)

Observed values outside the 95% confidence interval are shown in bold

Chapter VII

Discussion

This study statistically analyzed the cochlear volume of nine Krapina Neandertals to determine if Neandertals have similar sized cochleae compared to modern humans and extant apes. In light of Kirk and Gosselin-Ildari's (2009) recent description of the functional relationship between cochlear volume and the frequency limits of hearing in primates, the cochlear volume of Neandertals offers insight into their hearing abilities relative to modern humans. This study shows that Krapina Neandertals have the same absolute cochlear volume as modern humans, and significantly larger absolute cochlear volumes than chimpanzees and gorillas. According to Kirk and Gosselin-Ildari (2009), absolute cochlear volume is significantly negatively correlated with both the high and low frequency limits of hearing in primates. In other words, as cochlear volume increases, the range of audible frequencies shifts downward to lower frequencies. The current data suggest that Krapina Neandertals may have had the same range of audible frequencies as modern humans (from .031 to 17.6 kHz; Heffner, 2004), which is lower than the range of audible frequencies for chimpanzees and gorillas.

Kirk and Gosselin-Ildari (2009) also found that the high (but not low) frequency limit of hearing is significantly related to cochlear volume even when body mass is held constant. This means that species with relatively large cochleae for their body size also have relatively lower high frequency limits. In other words, at a given body size, species with larger cochleae have reduced high frequency limits compared to similar-sized species with smaller cochleae. Although this relationship is best illustrated by comparing the cochlear volume of two species of the same body mass, similar inferences for a single species can be made by comparing the cochlear volume predicted by body mass to the observed (measured) cochlear volume. For example, if a species has an observed cochlear volume that is larger than predicted by body mass (with linear regression), then the species would have lower high frequency limits than would be expected. The current finding that Neandertals and modern humans have larger cochleae than predicted by body mass (with OLS regression) indicates that both groups may have a reduced ability to hear high frequencies. However, the observed cochlear volume for Neandertals is just slightly greater than the 95% confidence interval with OLS regression and is within the 95% confidence interval with RMA regression (Table 6). This indicates that the difference between the observed and predicted cochlear volumes in Krapina Neandertals may represent statistical error rather than a true difference. Modern human cochlear volume, on the other hand, is above the 95% confidence interval with both OLS and RMA regression (Table 6). This finding, coupled with the result that Neandertal scaled cochlear volume is statistically smaller than modern human scaled cochlear volume (Table 5), indicates that a reduced high frequency limit of hearing (when compared to species of the same size) is less pronounced in Neandertals than modern humans.

As assessed by coefficients of variation, the variation of cochlear volume within the Krapina Neandertal sample (0.08) is not significantly different from the variation in the modern human sample (0.10). At this point, the implications of cochlear size variation are not clear. However, it is clear that differences in variation are unlikely due to age or sex differences because the human bony labyrinth reaches adult size between the 17th and 19th weeks of gestation (Jeffery and Spoor, 2004) and the length of the basilar membrane is not significantly different between human males and females (Miller, 2007).

Potential mechanisms for the relationship between cochlear volume and hearing ability

Kirk and Gosselin-Ildari’s (2009) used absolute cochlear volume as a proxy or substitute for basilar membrane length. Absolute cochlear volume negatively correlates with the high and low frequency limits of hearing, just as longer basilar membrane lengths are associated with increases in low-frequency sensitivity and decreases in high-frequency sensitivity (West, 1985; Echteler et al., 1994). A biological explanation for the relationship between longer basilar membranes (and associated increases in cochlear volume) and better low-frequency hearing may be that increases in basilar membrane length permit the spiral organ of Corti to accommodate more hair cells along its apical surface, where low frequencies are resolved (Gelfand, 2004). Additionally, given the significant relationship between cochlear volume and high frequency limit independent of body mass, cochlear volume itself may be functionally related to the high frequency limit of hearing. Though discussion of the various active and passive mechanical properties of the cochlea is beyond the scope of this study, it is reasonable to speculate that the mass of the fluid associated with increased cochlear size may have an effect on cochlear tuning. At this point, the precise mechanism(s) responsible for the observed relationship between cochlear volume and frequency limits remains unknown.

Implications for ecology and communication of Neandertals

The precise relationship between ecology and hearing ability is not well understood. Sound localization ability is one factor known to exert selective pressure on high frequency hearing in mammals (Masterson et al., 1969, Heffner, 2004). Mammals with small heads and consequently, short interaural distances (the distance between the ears), hear higher frequencies than mammals with large heads and large interaural distances (Masterson et al., 1969). The ability to detect high frequencies allows small mammals to localize sound using pinna cues and spectral differences between the ears (Heffner, 2004). Selective pressures for low-frequency hearing limits, on the other hand, are not readily apparent. Species with restricted low-frequency hearing tend to be small, and species with good low-frequency hearing tend to be large, but many exceptions exist (Heffner, 2004).

Variations in diet, predation, habitat, and communication are also important factors relating to hearing capability (de la Torre and Snowdon, 2002; Waser and Brown, 1986). Tarsiers, for example, have been known to capture insects with their eyes closed (Niemitz, 1979), perhaps relying on high frequency cues to located prey. A recent study confirmed that the Philippine tarsier (*Tarsius syrichta*) has a high-frequency limit within the ultrasonic range at 91 kHz (Ramsier et al., 2012). At the other end of the spectrum, it seems reasonable that large animals might be sensitive to lower frequency sounds to aid in hunting large prey. With respect to communication and habitat, blue monkeys *(Cercopithecus mitis*) use low-frequency, long-distance vocalizations that are adapted to the rainforest environment in which they live (Brown et al., 1995). Similarly, chimpanzees have W-shaped (bimodal) audiograms that depict two peaks of sensitivity, one at 8 kHz and another at 1 kHz (Coleman, 2009). Interestingly, chimpanzee pant-hoots for communication with conspecifics over long distances concentrate acoustic information at 1 kHz (Mitani et al., 1999). Unlike chimpanzees, humans show a U-shaped audiogram and do not exhibit a loss in sensitivity between 2 and 4 kHz (Coleman, 2009). Although a great deal of acoustic information in spoken language is concentrated in the regions up to 2.5 kHz (especially vowel sounds), the area between 2 and 4 kHz also contains relevant acoustic information for speech intelligibility (Fant, 1973). Spoken language is arguably the most important acoustic information in the human environment requiring humans to high sensitivity throughout the frequency range of spoken language.

Using outer and middle ear morphological parameters, Martinez et al. (2004) inferred that *Homo heidelbergensis* likely had hearing ability in the mid-range frequencies (2-4 kHz) similar to living humans. Given their phylogenetic relationship to *Homo heidelbergensis* (Arsuaga et al., 1993) it is probable that Neandertals also had similar hearing to modern humans in the middle frequencies. The current study uses an inner ear parameter (cochlear volume) to suggest that Neandertals had similar low and high frequency limits of hearing. Thus, the Neandertal audiogram would be very similar to modern humans in all respects: at the low frequency limit, midrange sensitivity, and at the high frequency limit. Though the evolutionary relationship between ecology and hearing sensitivity remains unclear, the similar hearing capabilities between Neandertals and modern humans suggest that both groups had similar ecological and communicative demands in their acoustic environments.

Future directions for the Krapina scans

The current study analyzed cochlear volume in Krapina Neandertals to shed light on their hearing ability as compared to modern humans and extant apes. Future study of additional cochlear measurements, such as cochlear length (Coleman and Colbert, 2010) or the ratio of the radii of curvature from the basal coil to the apical coil (Manoussaki et al., 2008), could be used to evaluate how other measures of cochlear size correspond to cochlear volume. Additionally, the current Krapina Neandertal sample contains three preserved stapes. Taxa with smaller stapedial footplate areas typically have enhanced high-frequency hearing, whereas taxa with large footplate areas are typically better at detecting low-frequency sounds (Rosowski, 1994). Thus, analysis of the Krapina stapes may offer further insight into their hearing abilities. Lastly, analysis of the semicircular canals of the Krapina Neandertals could be used to make inferences about their balance and locomotion.

Summary

In recent years it has become possible to infer hearing abilities in fossil specimens with preserved inner ear morphology. The current study examines cochlear volume in nine Krapina Neandertals with respect to modern human, chimpanzee, and gorilla comparative samples. This study shows that Krapina Neandertals have the same absolute cochlear volume as modern humans and significantly larger absolute cochlear volumes than chimpanzees and gorillas. Because increases in absolute cochlear volume are associated with decreases in the high and low limits of hearing (Kirk and Gosselin-Ildari, 2009) the data suggest that Krapina Neandertals may have had the same range of audible frequencies as modern humans, which is lower than the range of audible frequencies for chimpanzees and gorillas. Using both OLS and RMA regression, the observed cochlear volume of modern humans is larger than predicted by body mass. For the Krapnia Neandertals, cochlear volume is larger than predicted by body mass only when using OLS regression. Because species with relatively large cochleae for their body size have relatively lower high frequency limits (Kirk and Gosselin-Ildari, 2009), the current data suggest that modern humans may have a more pronounced reduction in high frequency hearing (relative to body size) than Neandertals. This study is the first to compare cochlear volume in Neandertals and modern humans, and adds to the small but growing body of literature surrounding the evolution of hearing in extinct taxa.

References

Armstrong, S. D., Bloch, J. I., Houde, P., Silcox, M. T., 2011. Cochlear labyrinth volume in Euarchontoglirans: implications for the evolution of hearing in primates. The Anatomical Record. 294, 263-266.

Arsuaga, J.L., Martinez, I, Gracia, A, Carretero, J.M., Carbonell, E., 1993. Three new human skulls from the Sima de los Huesos Middle Pleistocene site in Sierra de Atapuerca, Spain. Nature. 362, 534-537.

Békésy, G., 1960. Experiments in hearing. McGraw-Hill, New York.

Brace, C.L., 1964. The fate of the “classic” Neandertals: a consideration of hominid catastrophism. Current Anthropology. *5*, 3-43.

Brown, C.H., Gomez, R., Waser, P.M., 1995. Old world monkey vocalizations: adaptation to local habitat? Animal Behavior. 50, 945-961.

Caspari, R., Radovčić, J., 2006. New reconstruction of Krapina 5, a male Neandertal cranial vault from Krapina, Croatia. American Journal of Physical Anthropology. 130, 294–307.

Colelman, M.N., 2007. The functional morphology and evolution of the primate auditory system. Ph.D. Dissertation, Stony Brook, NY: Stony Brook University.

Coleman, M.N., 2009. What do primates hear? A meta-analysis of all known non-human primate behavioral audiograms. International Journal of Primatology. 30, 55-91.

Coleman, M. N., Colbert, M. W., 2010. Correlations between auditory structures and hearing sensitivity in non-human primates. Journal of Morphology. 271(5), 511–532.

Coleman, M. N., Kay, R. F., Colbert, M. W., 2010. Auditory morphology and hearing sensitivity in fossil new world monkeys. The Anatomical Record. 293(10), 1711–1721.

De la Torre, S., Snowdon, C.T., 2002. Environmental correlates of vocal communication in wild pygmy marmosets, *Cebulla pgymaea*. Animal Behavior. 63, 847-856.

Echteler, S.M., Fay, R.R., Popper, A.N., 1994. Structure of the mammalian cochlea. In: Fay, R.R., Popper, A.N., (Eds.), Comparative Hearing: Mammals. Springer-Verlag, New York, pp. 134-171.

Elder J.H., 1934. Auditory acuity of the chimpanzee. Journal of Comparative Psychology. 17, 157-183.

Fay, R., 1992. Structure and function in sound discrimination among vertebrates. In: Webster, D.B., Fay, R.R., Popper, A.N. (Eds.) The Evolutionary Biology of Hearing. Springer-Verlag, New York, pp. 229-263.

Fay, R., 1994. Comparative auditory research. In: Fay, R.R., Popper, A.N., (Eds.) Comparative Hearing: Mammals. Springer-Verlag, New York, pp. 1-17.

Fant, C.G.M., 1973. Speech Sounds and Features. MIT Press, Cambridge, MA.

Gelfand, S., 2004. Hearing: an Introduction to Psychological and Physiological Acoustics (4th ed.). Marcel Dekker, New York.

Gorjanović-Kramberger, D., 1906. Der diluviale Mensch von Krapina in Kroatia. Ein Beitrag zur Paläoanthropologie. Kreidel, Wiesbaden.

Gorjanović-Kramberger, D., 1913. Život i kultura diluvijalnoga čovjeka iz Krapine u Hrvatskoj. Djela Jugoslavenske Akademije Znanosti I Umjetnosti. 23, 1-54.

Greenwood, D.D., 1961. Critical bandwidth and the frequency coordinates of the basilar membrane. Journal of the Acoustical Society of America. 33, 1344-1356.

Greenwood, D.D., 1990. A cochlear frequency-position function for several species—29 years later. Journal of the Acoustical Society of America. 87, 2592-2605.

Heffner, R. S., 2004. Primate hearing from a mammalian perspective. The Anatomical Record Part A. 281(1), 1111–1122.

Hofman, M.A., Laan, A.C., Uylings, H.B.M., 1986. Bivariate linear models in neurobiology: problems of concept and methodology. Journal of Neuroscience Methods. 18,103-114.

Jeffery, N., Spoor, F., 2004. Prenatal growth and development of the modern human labyrinth. Journal of Anatomy. 204, 71-92

Kirk, E. C., Gosselin-Ildari, A. D., 2009. Cochlear labyrinth volume and hearing abilities in primates. The Anatomical Record. 292(6), 765–776.

Malez, M. 1978. Fossile Menschen aus Nordwestkroatien und ihre quartärgeologische, paläontologische und paläolithische Grundlage, Collegium Antropologicum. *2*, 29-41.

Manoussaki, D., Chadwick, R. S., Ketten, D. R., Arruda, J., Dimitriadis, E. K., O'Malley, J. T., 2008. The influence of cochlear shape on low-frequency hearing. Proceedings of the National Academy of Sciences. 105(16), 6162-6166.

Martínez, I., Rosa, M., Arsuaga, J. L., Jarabo, P., Quam, R., Lorenzo, C., Gracia, A., et al., 2004. Auditory capacities in Middle Pleistocene humans from the Sierra de Atapuerca in Spain. Proceedings of the National Academy of Sciences of the United States of America. 101(27), 9976-9981.

Masterson, B., Heffner, H., Ravizza, R., 1969. The evolution of human hearing. Acoustical Society of America. 45, 966-985.

Miller, J.D., 2007. Sex differences in the length of the organ of Corti in humans. Journal of the Acoustical Society of America. 121,151-155.

Milner G.W., Smith, V.G., 1990. Oneota human skeletal remains. In: Santure, S.K., Harn, A.D., Esarey, D., (Eds.) Archaeological Investigations at the Morton Village and Norris Farms 36 Cemetery. Illinois State Museum, Springfield, pp. 111-148.

Mitani, J, Hunley K, Murdoch M. 1999. Geographic variation in the calls of wild chimpanzees. American Journal of Primatology. 47, 133-151.

Moggi-Cecchi, J., Tobias, P.V., Beynon, A.D., 1998. The mixed dentition and associated skull fragments of a juvenile fossil hominid from Sterkfontein, South Africa. American Journal of Physical Anthropology. 106, 425-465.

Moggi-Cecchi, J., Collard, M., 2002. News and views: a fossil stapes from Sterkfontein, South Africa, and the hearing capabilities of early hominids. Journal of Human Evolution. 42, 259–265.

Ni, X., Flynn, J. J., Wyss, A. R., 2010. The bony labyrinth of the early platyrrhine primate *Chilecebus*. Journal of Human Evolution. 59(6), 595–607.

Niemitz, C., 1979. Outline of the behavior of *Tarsius bancanus*. In: Doyle, G.A., Martin, R.D., (Eds.), The Study of Prosimian Behavior. Academic Press, New York, pp. 631-660.

Purves, D., Augustine, G., Fitzpatrick, D., Katz, L., LaMantia, A.-S., McNamara, J. (Eds.), 1997. Neuroscience. Sinauer Associates, Sunderland Mass.

Quam, R., Rak, Y., 2008. Auditory ossicles from southwest Asian Mousterian sites. Journal of Human Evolution. 54(3), 414–433.

Radovčić, J., 1988. Dragutin Gorjanović-Kramberger and Krapina Early Man: the Foundation of Modern Paleoanthropology. Školsa Knjiga and Hrvatski Prirodoslovni Muzej, Zagreb.

Radovčić, J., Smith, F., Trinkhaus, E.,Wolpoff, M., 1988. The Krapina Hominids: an Illustrated Catalog of the Skeletal Collection. Mladost Press and the Croatian Natural History Museum, Zagreb.

Rak, Y, Clarke, R.J., 1979. Ear ossicle of *Australopithecus robustus.* Nature. 279, 62-63.

Ramsier, M.A., Cunningham, A.J., Moritz, G.L., Finneran, J.J., Williams, C.V., Ong, P.S., Gursky-Doyen, S.L., Dominy, N.J., published ahead of print February 8, 2012. Primate communication in the pure ultrasound. Biological Letters. doi:10.1098/rsbl.2011.1149

Rink, W., Schwarcz, H., Smith, F., Radovčić, J., 1995. ESR ages for Krapina hominids. Nature. 378, 24.

Rosowski, J., 1994. Outer and middle ears. In: Fay, R.R., Popper, A.N. (Eds.) Comparative Hearing: Mammals. Springer-Verlag, New York. pp. 172-247.

Ruff, C.B., Trinkhaus, E., Holliday, T.W., 1997. Body mass and encephalization in Pleistocene *Homo*. Nature. 387, 173-176.

Samuels, M.L., Witmer, J.A., 2003. Statistics for the Life Sciences. Pearson Education, Inc. Upper Saddle River, New Jersey.

Silcox, M. T., Bloch, J. I., Boyer, D. M., Godinot, M., Ryan, T. M., Spoor, F., Walker, A., 2009. Semicircular canal system in early primates. Journal of Human Evolution. 56(3), 315–327.

Spoor, F., Zonneveld, F., 1995. Morphometry of the primate bony labyrinth: a new method based on high-resolution computed tomography. Journal of Anatomy. 186, 271-286.

Spoor F., Zonneveld, F., 1998. Comparative review of the human bony labyrinth. Yearbook of Physical Anthropology. 41, 211-251.

Spoor, F., Hublin, J. J., Braun, M., Zonneveld, F., 2003. The bony labyrinth of Neanderthals. Journal of Human Evolution. 44(2), 141–165.

Spoor F., Garland, T. Jr., Krovitz. G., Ryan, T.M., Silcox, M.T., Walker, A., 2007. The primate semicircular canal system and locomotion. Proceedings of the National Academy of Sciences of the United States of America. 104(26), 10808-10812.

Smith, F., 1976. The Neandertal remains from Krapina: a descriptive and comparative study. University of Tennessee Department of Anthropology Report of Investigation. 15, 1-359.

Smith, R.J., 1994. Regression models for prediction equations. Journal of Human Evolution. 26, 239-244.

Smith, R.J., 2009. Use and misuse of the reduced major axis for line-fitting. American Journal of Physical Anthropology. 140, 476-486.

Smith, R.J., Jungers, W.L., 1997. Body mass in comparative primatology. Journal of Human Evolution. 6, 523-559.

Warton, D.I., Wright, I.J., Falster, D.S., Westoby, M., 2006. Bivariate line-fitting methods for allometry. Biological Reviews. 81, 259-291.

Waser, P.M., Brown, C.H., 1986. Habitat acoustics and primate communication. American Journal of Primatology. 10, 135-154

West, C.D., 1985. The relationship of the spiral turns of the cochlea and the length of the basilar membrane to the range of audible frequencies in ground dwelling mammals. Journal of the Acoustical Society of America. 77, 1091-1101

Wolpoff, M. H., 1979. The Krapina dental remains. American Journal of Physical Anthropology. 50(1), 67–113.

APPENDIX A. Chimp and Gorilla Cochlear Labyrinth Volumes by Segmenting Method

Specimen	Species	"Low Threshold" Cochlear Volume (mm^3)	"High Threshold" Cochlear Volume (mm^3)	"Low-High Threshold Average" Cochlear Volume (mm^3)	"Eyeball" Cochlear Volume (mm^3)	Percent Difference between "Threshold Average" and "Eyeball" volumes
AMNH 54330 (m)	*Pan troglodytes*	43.21	49.38	46.29	47.56	2.66
AMNH 90191 (f)	*Pan troglodytes*	43.65	51.34	47.49	48.86	2.79
AMNH 167343 (f)	*Pan troglodytes*	46.31	57.70	52.00	52.65	1.23
AMNH 167344 (m)	*Pan troglodytes*	67.53	72.39	69.96	69.49	0.68
AMNH 167346 (m)	*Pan troglodytes*	57.75	63.26	60.50	61.34	1.36
AMNH 167330 (f)	*Gorilla gorilla*	55.99	63.44	59.72	60.34	1.04
AMNH 167337 (f)	*Gorilla gorilla*	51.88	58.28	55.08	55.73	1.17
NMNH 176210 (m)	*Gorilla gorilla*	62.70	66.10	64.40	65.07	1.04
NMNH 176216 (m)	*Gorilla gorilla*	69.20	75.03	72.11	72.32	0.29
NMNH 176220 (m)	*Gorilla gorilla*	57.25	67.54	62.39	63.55	1.82

APPENDIX B. Manual segmenting reliability check

Specimen	Species	First Pass Cochlear Volume (mm^3)	Second Pass Cochlear Volume (mm^3)	Percent Difference
Norris Farms 820227	*Homo sapiens*	87.88	86.47	1.61
Norris Farms 820696	*Homo sapiens*	68.3	64.89	5
Norris Farms 821205	*Homo sapiens*	71.55	72.09	0.75